TAMPEREEN TEKNILLINEN YLIOPISTO
TAMPERE UNIVERSITY OF TECHNOLOGY

VESA AHO

INSOLE ENERGY HARVESTING FROM HUMAN MOVEMENT USING PIEZOELECTRIC GENERATORS

Master of Science Thesis

Examiners:
Asst. Prof. Sampo Tuukkanen,
Lec. Risto Mikkonen
Examiners and topic approved on 9th August 2017

ABSTRACT

VESA AHO: Insole energy harvesting from human movement using piezoelectric generators
Tampere University of Technology
Master of Science Thesis, 62 pages
February 2018
Master's Degree Programme in Electrical Engineering
Major: Renewable Electrical Energy Technologies
Examiners: Assistant Professor Sampo Tuukkanen, Lecturer Risto Mikkonen

Keywords: piezoelectricity, energy harvesting, shoes, human movement, walking, piezoelectric diaphragms

The energy requirements of various sensors and portable devices are conventionally met with batteries that have limited lifetimes and contain hazardous materials. Different energy harvesting technologies have emerged as possible alternatives to batteries. With these technologies energy that would otherwise be wasted, can be transformed into useful electric energy to power some applications. There are many readily available energy sources that can be exploited. One of them is different forms of mechanical energy that can be captured with piezoelectric energy harvesters. Several watts of energy can potentially be captured from walking without interfering with the normal gait by integrating piezoelectric energy harvesters in shoes.

In this thesis energy harvesting from walking with piezoelectric energy harvesters is discussed by presenting the basic concepts and theory behind piezoelectric energy harvesting, and providing a literature review about various existing shoe energy harvester designs. Inspired by these designs a piezoelectric shoe energy harvester is developed using commercially available components and its capability to harvest energy is demonstrated.

TIIVSTELMÄ

VESA AHO: Insole energy harvesting from human movement using piezoelectric generators
Tampereen teknillinen yliopisto
Diplomityö, 62 sivua
Helmikuu 2018
Sähkötekniikan diplomi-insinöörin tutkinto-ohjelma
Pääaine: Uusiutuvat sähköenergiateknologiat
Tarkastajat: Apulaisprofessori Sampo Tuukkanen, Lehtori Risto Mikkonen

Avainsanat: pietsosähköisyys, energian louhinta, energiankeräys, kengät, käveleminen, pietsosähköiset elementit

Erilaisten sensoreiden ja kannettavien elektronisten laitteiden tarvitsema energia on tavallisesti tuotettu paristoilla. Paristoilla on kuitenkin rajallinen elinikä, jonka jälkeen ne ovat ongelmajätettä. Erilaisilla energian louhintamenetelmillä voidaan mahdollisesti pidentää paristojen elinikää tai poistaa ne kokonaan. Energian louhinnalla voidaan kerätä pieniä määriä energiaa erilaisista pienistä energianlähteistä, joita esiintyy kaikkialla ympäristössä. Pietsosähköisten materiaalien avulla voidaan muuntaa monenlaista mekaanista energiaa sähköenergiaksi. Tätä mekaanista energiaa voidaan louhia mm. kävelemisestä asentamalla pietsosähköisiä elementtejä kenkiin. Eräiden tutkimusten mukaan kävelemisestä voidaan louhia useampia watteja häiritsemättä normaalia kävelyä.

Tässä diplomityössä perehdytään energian louhintaa kävelemisestä pietsosähköisillä elementeillä esittelemällä pietsosähköisen ilmiön keskeisimpiä käsitteitä ja teoriaa sekä tekemällä kirjallisuusselvitys olemassa olevista kenkiin asennetuista pietsosähköiseen ilmiöön perustuvista energiaharvestereista. Lisäksi rakennetaan vastaavanlainen energiaharvesteri kaupallisista komponenteista ja demonstroidaan sen avulla energian louhintaa kävelemisestä.

PREFACE

This thesis work was done for Nokia Technologies in the Faculty of Biomedical Sciences and Engineering at Tampere University of Technology. I would like to thank everyone who contributed to the accomplishment of this thesis.

Tampere, 27.2.2018

Vesa Aho

CONTENTS

LIST OF FIGURES

LIST OF TABLES

LIST OF SYMBOLS AND ABBREVIATIONS

MFC	Micro fiber composite
PFC	Piezoelectric fiber composite
PMN-PT	Lead magnesium niobate-lead titanate
PVDF	Polyvinylidene fluoride
PZT	Lead zirconate titanate
PZT-PT	lead zinc niobate-lead titanate
RFID	Radio frequency identification
SSHI	Switch harvesting on inductor
THUNDER	Thin Layer UNimorph Ferroelectric DriVER and Sensor

BW	bandwidth
C	capacitance
C_0	capacitance of PZT ceramic measured at a frequency of 100 Hz
C_p	parallel capacitance
C_{RECT}	voltage over output capacitance
d	piezoelectric charge coefficient
D	dielectric displacement
E	electric field
f	operating frequency
f_r	resonant frequency
g	piezoelectric voltage coefficient
k^2	piezoelectric coupling coefficient
q	charge
Q	mechanical quality factor
R_p	parallel resistance
S	strain
s^E	compliance under constant electric field
T	stress
V	voltage
V_D	voltage drop over diode
V_{RECT}	rectifier output voltage
Z	approximated optimal resistance
ε	dielectric constant
ε_0	vacuum permittivity
ε^T	dielectric constant under constant stress

1. INTRODUCTION

Capturing small amounts of energy, that would otherwise be lost as heat, light, sound or movement, from the environment and converting it into electricity is called energy harvesting (IOP n.d.). This energy can be used to power low power electronics that are conventionally powered with batteries or it can be used to extend the lifetime of batteries. In the surroundings there are several energy sources that can be exploited. These include mechanical energy in various forms of movements and vibrations, electromagnetic energy, thermal and pressure gradients, solar, etc (Harb 2010). The energy can be harvested with different methods depending on the type of energy source available. A promising approach to energy harvesting is to use piezoelectric materials to transform mechanical energy into electrical energy.

Piezoelectricity was discovered in 1880 by Curie brothers when they noticed that applying mechanical force to certain materials will induce an electric field. Next year the reverse effect was also discovered. (Kholkin et al. 2008) One of the first practical applications to use piezoelectricity was the SONAR system used in submarines (Piezo systems n.d.) but only after the Second World War industries developing piezoelectric systems started to scale up and are today multimillion dollar industries (Kholkin et al. 2008). A more detailed review of the history of piezoelectricity is provided by Uchino. (Uchino 2010) In the past decades piezoelectric materials have received interest as generators in energy harvesting applications.

The recent trend in the field of electronics has been the decrease of the size and power consumption of electronic components and devices. This has enabled the creation of new applications that have very low power requirements. In some of these applications, the use of traditional batteries is not an optimal solution because the batteries have a limited energy content and replacing them can be difficult and costly. This has led to a search for alternative ways to power the applications and spurred the research of piezoelectric energy harvesting.

An interesting concept of piezoelectric energy harvesting is to exploit the mechanical energy of human movement. According to Starner and Paradiso one of the largest and most readily available source of mechanical energy in human movement is the energy associated with footstrikes during walking or running (Starner and Paradiso 2004). This finding has inspired researchers to find ways to make use of this energy with shoe energy harvesters of various designs. The state of the art unobtrusive piezoelectric shoe energy harvesters today can generate more than 10 mJ of raw energy each step during walking (Wang 2010, Leinonen et al. 2016).

The aim of this thesis is to provide a literature review of piezoelectric shoe energy harvesters, to demonstrate energy harvesting from walking with a harvester build from commercial components, and find out how much energy is possible to harvest with the developed design. Piezoelectric diaphragms made from lead zirconate titanate (PZT) piezoelectric ceramic were chosen as the piezoelectric elements because they are widely available, low cost and have relatively good piezoelectric response.

The construction of this thesis is the following. In Chapter 2 the origin of piezoelectricity and the basic mathematical relations in piezoelectric materials are presented. In Chapter 3 different piezoelectric materials, rectifiers, and energy storages for energy harvesting systems are discussed. In Chapter 4 various piezoelectric shoe energy harvester designs are presented. In Chapter 5 the developed shoe energy harvester is presented along with the related experiments. In Chapter 6 the results and possible applications for shoe energy harvesters are discussed.

2. PIEZOELECTRICITY

This section provides a brief overview of the relevant theoretical concepts of piezoelectricity.

2.1 Origin of piezoelectricity

The origin of piezoelectricity is in the molecular structure of the material. Crystals can be divided into 32 classes of which 21 do not have a center of symmetry. When a force is applied to crystals of these 21 classes a net movement of positive and negative ions occurs during the deformation and an electric dipole is formed. This is illustrated in Figure 1. In crystals having a center of symmetry the net movement of ions is zero and dipoles will not be formed. The net movement is zero also in one of the 21 classes due to a combination of other symmetry elements. (Ouyang 2005)

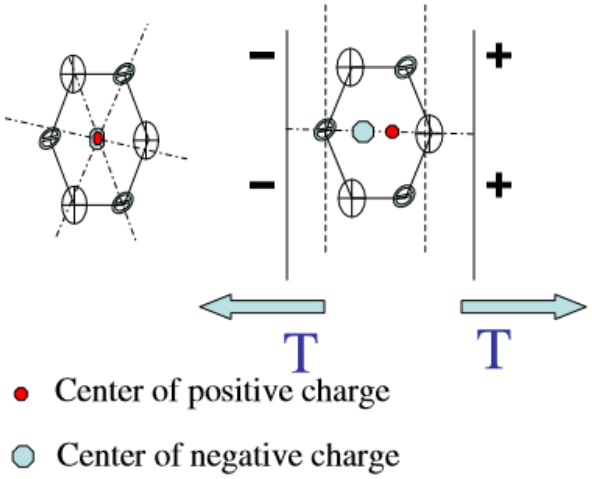

Figure 1. *Formation of a dipole in piezoelectric crystal under tensile stress. (Ouyang 2005)*

Some materials, for instance quartz and tourmaline single crystals, are naturally piezoelectric. Some materials can be made piezoelectric. One of the most widely used piezoelectric material, PZT, is a polycrystalline material that is composed of randomly oriented dipoles. When the material is deformed, the piezoelectric effect of the different dipoles cancel each other and the net piezoelectric effect is weak. When this material is placed in a strong DC electric field, the dipoles become oriented to the same direction. When the electric field is removed, the dipoles will roughly have the same orientation and will exhibit a strong piezoelectric effect when deformed. Orienting the dipoles with electric field is called poling and is illustrated in Figure 2. (Panda 2017) If poled piezoelectric ceramics are heated above a certain temperature, known as the Curie temperature, it loses its piezoelectricity. Depolarization can occur also when electric field

of opposite polarity is applied to the material, or when mechanical stress on the material becomes high enough. (Morgan Advanced Materials n.d.)

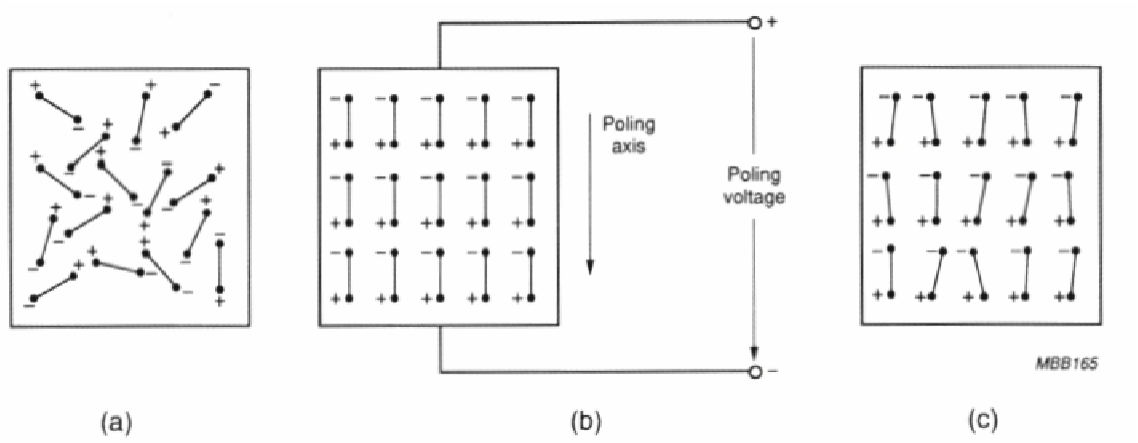

Figure 2. *Poling of piezoelectric materials. (a) Before poling (b) during poling (c) after poling. (Morgan Advanced Materials n.d.)*

2.2 Constitutive equations

The constitutive equations of piezoelectricity are a simplified mathematical model that represents the electromechanical coupling in piezoelectric materials. In the model the electromechanical coupling is assumed to be linear and is presented by coupling coefficients. There are different forms and notations for the constitutive equations. A frequently used notation is shown in Equations

$$S = s^E T + dE \tag{1}$$

$$D = dT + \varepsilon^T E, \tag{2}$$

where S is strain, T is stress, s^E is compliance under constant electric field, d is piezoelectric charge coefficient, ε^T is dielectric constant under constant stress, E is electric field and D is electric displacement. S, T and ε^T are second rank tensors, s^E is a fourth rank tensor, d is a third rank tensor, and E and D are vectors. (Jordan and Ounates 2001).

The direct piezoelectric effect is described with the Equation 2, that is also known as the sensor equation, where the input is mechanical energy and the output is electrical energy. In general, the mechanical input can be in the form of external stress or strain and the electrical output can be in the form of surface charge density, electric field or voltage. In the indirect effect, described by the Equation 1, also known as the actuator equation, the input and output forms are the opposites compared to the Equation 2 (Abramovich 2016).

If d equals zero, the equations present the properties of a non-piezoelectric linear material.

2.3 Piezoelectric coefficients

Because the piezoelectric effect is anisotropic, i.e. the piezoelectric properties are directionally dependent, it is described by tensors. The piezoelectric effect is inherently transient and therefore the piezoelectric coefficients can be defined with partial derivatives. The piezoelectric coefficients have several forms depending what units are used in the constitutive equations. The piezoelectric coefficient *d*, that is known as the piezoelectric charge coefficient, given in [C/N] can be defined for the direct effect as

$$d = \frac{\partial D}{\partial T} \tag{3}$$

and for the indirect effect as

$$d^* = \frac{\partial S}{\partial E}\,. \tag{4}$$

With thermodynamics it can be proved that *d* equals *d**. (Abramovich 2016)

Piezoelectric coefficient *g*, that is known as the piezoelectric voltage coefficient, given in [V·m/N], is another way to present the piezoelectric effect. It links the electric field and the stress with the equation (Abramovich 2016)

$$g = -\left(\frac{\partial E}{\partial T}\right)_D. \tag{5}$$

Piezoelectric voltage constant *g* is related to the charge constant *d* with the equation

$$g = \frac{d}{\varepsilon_0 \varepsilon}\,, \tag{6}$$

where ε is the dielectric constant of the material and ε_0 is the vacuum permittivity. (Rogers and Wallace 1994)

2.4 Reduced matrix notation

In some materials, due to crystal symmetries, the number of independent components in tensors can be reduced by the choice of reference axes. A convenient choice of reference axes is shown in Figure 3. The poling direction is chosen as axis 3 and the perpendicular directions as axes 1 and 2. The shear planes of the axes are indicated by subscripts 4, 5 and 6. (Jordan and Ounates 2001)

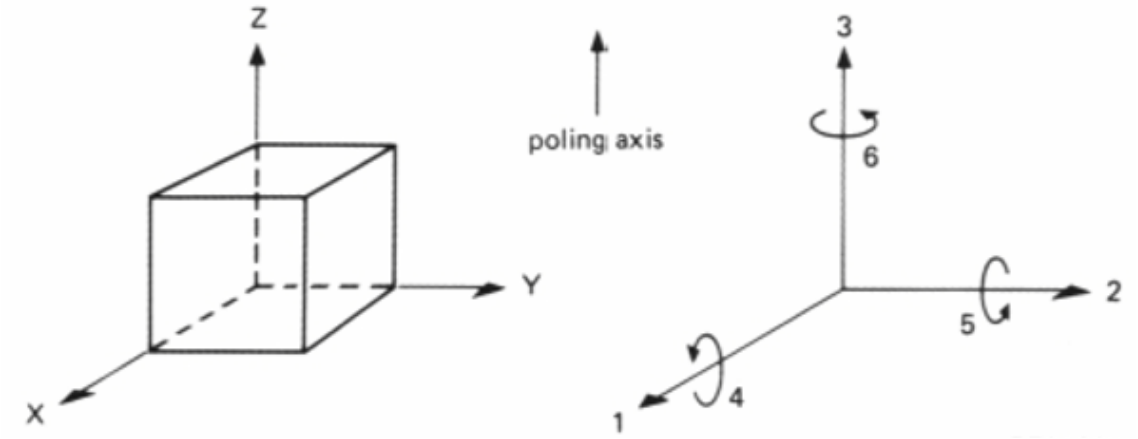

Figure 3 *Reference axes for reduced matrix notation. (Morgan Advanced Materials n.d.)*

When the axes are chosen as described, a reduced matrix notation for the second rank tensors S_{ij} and T_{ij} can be used. The indices i and j, taking values from 1 to 3, can be replaced by a single index taking values from 1 to 6 as shown below.

$$\begin{gathered} 11 \equiv 1 \\ 22 \equiv 2 \\ 33 \equiv 3 \\ 23 = 32 \equiv 4 \\ 31 = 13 \equiv 5 \\ 12 = 21 \equiv 6 \end{gathered} \tag{7}$$

The subscripts 1, 2 and 3 indicate the direction of normal tensile/compressive stress or strain and the subscripts 4, 5 and 6 indicate the direction of shear stress or strain as shown in the Figure 3. (Abramovich 2016)

In the same manner, the piezoelectric d coefficient can be presented by a 3 x 6 matrix as shown below (Abramovich 2016). The first subscript of the components refers to the direction of the applied or induced electric field and the second subscript refers to the direction of the applied or induced stress or strain. (Morgan Advanced Materials n.d.)

$$\begin{pmatrix} d_{11} & d_{12} & d_{13} & d_{14} & d_{15} & d_{16} \\ d_{21} & d_{22} & d_{23} & d_{24} & d_{25} & d_{26} \\ d_{31} & d_{32} & d_{33} & d_{34} & d_{35} & d_{36} \end{pmatrix} \tag{8}$$

In some cases the matrix can be further reduced. Due to the specific crystal structure of PZT, and assuming that the piezoelectric ceramic is isotropic in a plane perpendicular to the poling direction, several terms in the piezoelectric coefficient matrix will become zero or equal to each other. According to Kholkin *et al.* tetragonal crystals of the 4 mm symmetry and poled ceramics have only three independent components in their piezoelectric *d* coefficient and can be presented with matrix shown below. (Kholkin et al. 2008)

$$\begin{pmatrix} 0 & 0 & 0 & 0 & d_{15} & 0 \\ 0 & 0 & 0 & d_{15} & 0 & 0 \\ d_{31} & d_{31} & d_{33} & 0 & 0 & 0 \end{pmatrix} \tag{9}$$

In addition to the piezoelectric *d* and *g* coefficients, piezoelectric elements can be characterized with the piezoelectric coupling coefficient, *k,* and the mechanical quality factor, Q_m.

2.5 Piezoelectric coupling coefficient

Piezoelectric coupling coefficient quantifies the piezoelectric element's capability to convert mechanical energy to electrical energy and vice versa. It can be defined as

$$k^2 = \frac{E_{stored}}{E_{in}}, \tag{10}$$

where E_{stored} is the stored mechanical or electrical energy and E_{in} is the input electrical or mechanical energy. (Uchino 2000)

It can be also presented in terms of piezoelectric *d* coefficient, compliance under constant electric field, and dielectric constant under constant stress, ε^T (Abramovich 2016)

$$k^2 = \frac{d^2}{\varepsilon^T s^E}. \tag{11}$$

To take into account the directional dependency, the piezoelectric coupling coefficient is typically presented with the same notations as used for the piezoelectric *d* coefficient.

2.6 Mechanical quality factor

Piezoelectric elements generate their maximum powers at a specific frequency called the resonant frequency. Mechanical quality factor indicates how sharp the resonance peak is (see Figure 4). (Li et al. 2014) It can be defined as

$$Q = \frac{f_r}{BW}, \tag{12}$$

where f_r is the resonant frequency and BW is the bandwidth, that is the range of frequencies where the response is at least one half of the maximum response. (Piezo Technologies n.d.)

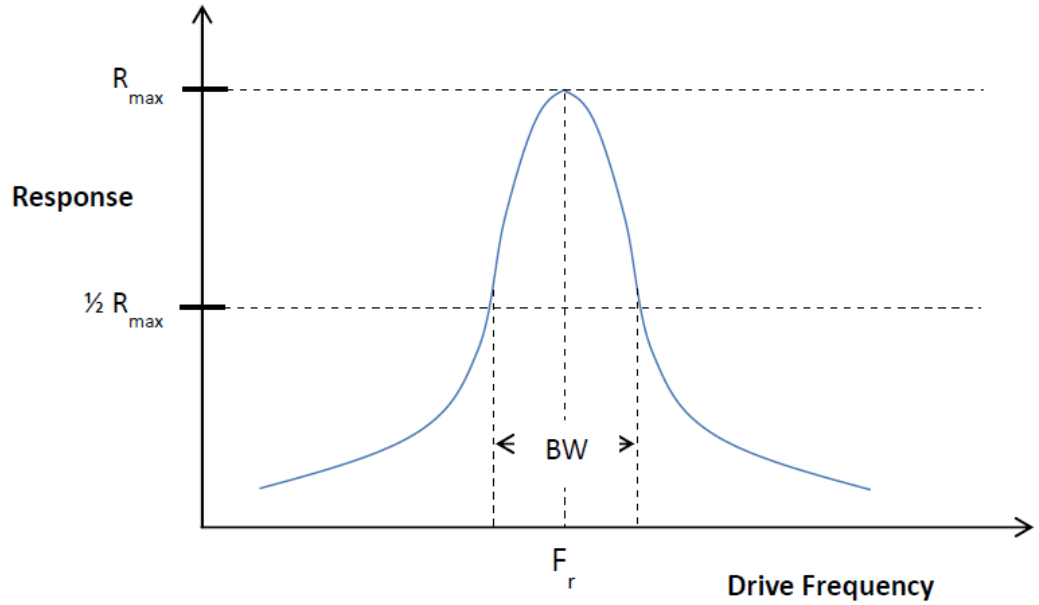

Figure 4. *Defining mechanical quality factor with bandwidth. (Piezo Technologies n.d.)*

For low-frequency applications, like the shoe energy harvesters, the mechanical quality factor is rather unimportant since they work outside the resonance.

The piezoelectric equations are simplifications and do not take all possible factors into account. In reality the piezoelectric relations are not entirely linear. Also factors such as temperature and the way crystals are cut can effectively change the piezoelectric coefficients. Close to the Curie point the piezoelectric coefficients are typically much larger. (Kholkin et al. 2008)

3. PIEZOELECTRIC MATERIALS, RECTIFIERS AND ENERGY STORAGES FOR ENERGY HARVESTING

This section provides a brief overview of the most common piezoelectric materials, and of different rectifiers and energy storages used in energy harvesting.

3.1 Piezoelectric materials

Li *et al.* have published a very compact overview of piezoelectric energy harvesting and piezoelectric materials. They divide piezoelectric materials to four groups based on their structural characteristics: single crystals, ceramics, polymers and composites. (Li et al. 2014)

Single crystals have good piezoelectric properties because the dipoles are organized in a periodic fashion throughout these materials resulting in a strong polarization in their structure. Lead magnesium niobate-lead titanate solid solution (PMN-PT) and lead zinc niobate-lead titanate PZN-PT have the best piezoelectric properties and are most widely used among single crystals. The disadvantage of single crystals is that they are rigid and brittle making them unsuitable for some applications. (Li et al. 2014)

Piezoelectric ceramics are polycrystals that can be made piezoelectric by poling. The most typical piezoelectric ceramics used in energy harvester applications are based in PZT because they are low cost, and have good piezoelectric properties and high Curie temperature. There are many types of PZT based materials, such as PZT4, PZT5-A, PZT-5H, PZT-7D, and PZT-8. All of them have slightly different physical properties (Kutz 2016). The most used are PZT-5H and PZT-5A. Also ceramics have the disadvantage of being rigid and brittle. Furthermore, PZT is highly toxic due to its lead content. (Jain et al. 2015)

PVDF is the most widely used piezoelectric polymer. It consists of repeating units of (CH_2-CF_2) (Li et al. 2014). The most significant advantage of PVDF compared to ceramics is that they are flexible, robust, and chemically inert. They can be easily placed on curved surfaces and bent, which makes them good materials for wearable items. The disadvantage is that they have much lower piezoelectric and dielectric coefficients. (Jain et al. 2015) Some researchers also consider PVDF's fluorine content, that is potentially toxic substance, a great disadvantage (Lekkala et al. 2003).

Piezoelectric composites are made by combining materials from different groups. The idea is to achieve flexibility together with good piezoelectric properties, achieving one

will usually come at the expense of the other. PVDF-PZT, "Piezoelectric fiber composites" (PFC) and "Micro Fiber Composite" (MFC) are examples of composites that have been developed. (Li et al. 2014, Jain et al. 2015)

Table 1 shows some of the key parameters of selected piezoelectric materials from different groups.

Table 1. *Parameters of selected piezoelectric materials. Adapted from (Li et al. 2014).*

	PZT-5H (ceramic)	PMN-32PT (single crystal)	PZT rod-Polymer composite with 30 vol. % PZT	PVDF (polymer)
Density (g/cm3)	7,65	8,1	3,08	1,78
Dielectric constant εr	3250	7000	380	6
Young's modulus Y33 (Gpa)	71,4	20,3		2
Mechanical quality factor Qm	32			10
Piezoelectric charge constat d33 (pC/N)	590	1620	375	25
Piezoelectric charge constat d31 (pC/N)	-270	-760		12-23
Electromechanical coupling coefficient k33	0,75	0,93		0,22

3.2 Rectification circuits

In addition to piezoelectric elements, the energy harvesting circuit consists of an AC-DC rectifier and an energy storage. Often some type of voltage regulator is also used to improve the power extraction. According to Ottman *et al.* using a DC-DC converter the power transfer to a battery can be increased by 400 % (Ottman et al. 2002). The research on efficient rectifiers is ongoing and various designs have been proposed. As a simple AC-DC rectifier some researchers use a half wave rectifier but the most common rectifier in energy harvesting studies, some times referred as standard interface, is a full bridge rectifier made of four diodes. Because it is inherently inefficient other types of rectifiers and additional converters have been developed based in different technologies. A logical next step from diode based bridge rectifiers is to use active components instead of diodes. Nielsen-Lönn *et al.* have investigated different kind of active rectifiers that use CMOS technology (Nielsen-Lonn et al. 2015).

Guyomar *et al.* presented a technique called synchronized switch harvesting on inductor (SSHI) that was reported to provide 900% increase in output power compared with a standard energy harvesting circuit (Guyomar et al. 2005). Since then several synchronized switching circuit topologies have been proposed. The inductor can be connected in parallel or in series with the piezoelectric element and is called accordingly parallel-SSHI and series-SSHI. The switch can be placed between the piezoelectric element and the rectifier or the rectifier and the storage buffer. (Liu and Vasic 2012)

Ramadas *et al.* presented one type of SSHI called the "bias flip" rectifier and compared its output to a conventional full bridge rectifier and a voltage doubler. The equivalent circuits of the full bridge and bias flip rectifiers are shown in Figures 5 and 6. The piezoelectric element is presented as a current source in parallel with a capacitance C_p and a resistance R_p. According to Ramadass *et al.* in full bridge rectifiers and voltage doublers the output is limited by the charging and discharging of C_p. In full bridge rectifiers when the current pulse changes from negative to positive it has to first discharge C_p from the voltage $-(V_{RECT}+2V_D)$ determined by the output voltage V_{RECT} and the voltage drop over the diodes V_D, and then charge it with the opposite charge to $V_{RECT}+2V_D$ before the rectifier starts to conduct. When using voltage doublers, C_p has to charge to $V_{RECT}+V_D$. To overcome these limitations a simple switch, M1, was connected across the piezoelectric element to discharge C_p at zero crossing. This configuration is called a "switch-only" rectifier. To further improve the rectifier an inductor is connected in series with the switch to passively flip the voltage of C_p. This configuration is called the bias-flip rectifier. (Ramadass and Chandrakasan 2010)

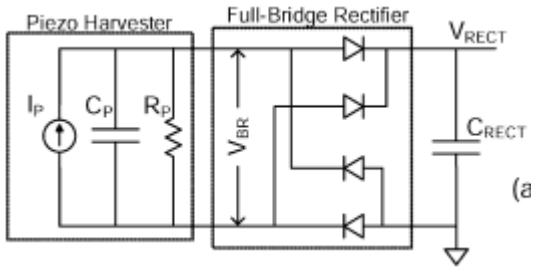

Figure 5. *Equivalent circuit of a piezoelectric element with a full bridge rectifier and an output capacitor. (Ramadass and Chandrakasan 2010)*

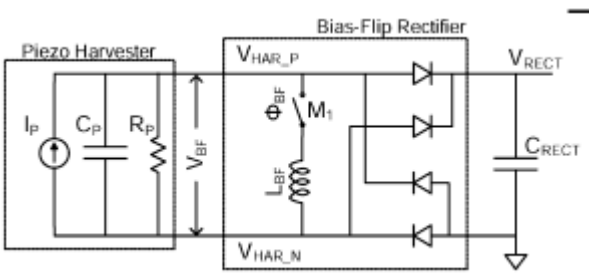

Figure 6. *Equivalent circuit of a piezoelectric element with the bias-flip rectifier. (Ramadass and Chandrakasan 2010)*

The switch is operated with a control circuit that is driven by a DC-DC boost converter. A DC-DC buck converter was used to transfer energy more efficiently to a storage capacitor. The problem with the bias-flip rectifier is that the inductor should be matched with the input capacitance that can require inductances of several Henrys, which is impractical. Compared to full bridge rectifier the authors were able to demonstrate more than 4x and 8x improvement in the power extracted to a storage capacitor with off-chip

and on-chip diodes respectively using the bias flip rectifier. (Ramadass and Chandrakasan 2010)

Improvement of this rectifier design has been demonstrated to increase the performance by 22x compared with a full bridge rectifier (Du et al. 2017).

Not all the demonstrations have been as successful. Wang implemented a series-SSHI including a peak detecting circuit, a buck converter and a BiMOS switch but the circuit only increased the maximum power output by 10-20 % compared with a full bridge rectifier. The circuit is shown in Figure 7. (Wang 2010)

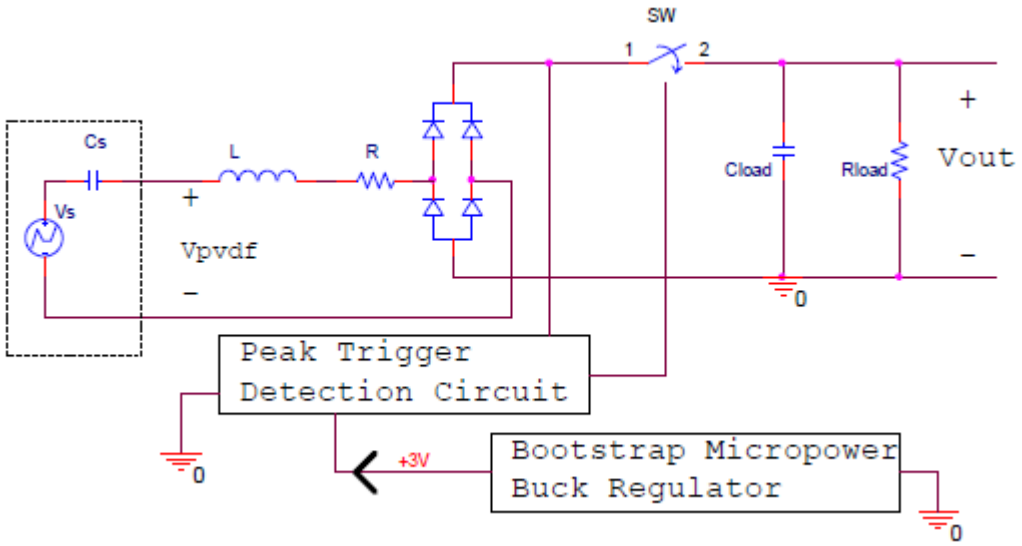

Figure 7. *Circuit diagram of a series-SSHI rectifier. (Wang 2010)*

The problem with these elaborated rectifier designs is that the converters and control circuits consume energy and that the inductor makes them unsuitable for CMOS integration. This problem is addressed by Lu *et al.* in their design of an inductorless self-controlled rectifier (Lu and Boussaid 2015).

In additions, there are some integrated circuits, such as the LTC3588–1 by Linear Technology and Texas Instruments' BQ25505, with rectification commercially available for energy harvesting. (Li et al. 2014)

3.3 Energy storages

Because the power outputs of piezoelectric energy harvesters are very low and the energy is not enough to power most electronic devices directly, the energy must be accumulated to a storage before usage. The conventional energy storages for energy harvesting applications have been capacitors.

Capacitors do not require any minimum voltage to start charging which makes them easy to charge and discharge fast. However, they have quite low energy densities and their

self-discharge rates are high which makes them unsuitable for some applications. (Li et al. 2014) For these reasons, some researchers favor rechargeable batteries as energy storages. According to Sodano *et al.* capacitors are fundamentally not well suited for energy storage and in order to commercialize energy harvesters rechargeable batteries should be used. (Sodano et al. 2005)

The problem with rechargeable batteries is that they are subjected to limited charging cycles (300-1000) after which they become hazardous waste. In addition, rechargeable batteries generally require relatively large currents to charge up efficiently which is not possible with the energy harvesters (Roundy 2003). Recently supercapacitors have been explored in order to overcome the shortcomings of capacitors and rechargeable batteries. Supercapacitors store energy by means of an electrolyte solution between two solid conductors, which gives them a greater capacitance and energy density compared with the conventional capacitors (Chen et al. 2009). They can have charge/discharge cycles up to a million. (Li et al. 2014)

Guan *et al.* compared the suitability of rechargeable batteries and supercapacitors as energy storages for piezoelectric energy harvesters in their research. The suitability was evalutated based on charge/discharge efficiency, adaptability to piezoelectric energy harvesting circuit, lifetime, and charge protection circuit of the energy storage devices. They concluded that supercapacitors are suitable and more desirable than the rechargeable batteries to store the energy in the piezoelectric energy harvesting systems. (Guan and Liao 2008) In some applications also combining supercapacitors and rechargeable batteries can be considered (Tolentino and Talampas 2012).

4. PIEZOELECTRIC ENERGY HARVESTING SHOES

Various piezoelectric energy harvesting shoes have been developed in the past two decades. The developers have considered in their design not only maximizing the output but also making the harvester unobtrusive. To be able to compare the piezoelectric elements of different designs, researchers have often determined the raw power of the harvester i.e. a RMS power to an optimal resistor connected to the piezoelectric element directly or through a rectifier. Some researcher also emphasize the power density of their piezoelectric element as a key criterion. Often the energy harvesters combine two different elements or stack same type of elements. The literature review of the existing piezoelectric shoe energy harvesters is provided in this section.

4.1 Hydraulic system

One of the first piezoelectric shoe energy harvesters was developed by Antaki *et al.* It was made of piezoelectric stacks that were housed in two cylinders under the foot and was actuated by hydraulic amplifiers at each end as shown in Figure 8. The force of the step is divided to smaller "packets" using a hydraulic oscillator that converts the stroke from step to pulses which have a frequency five times that of the stroke. The power was reported to depend on the weight of the user and the walking frequency. Average power levels of 256-676 mW for walking and 676-2100 mW for running were achieved with test persons weighting 52-75 kg using matched electric load with a full bridge rectifier and a buffer capacitor. (Antaki et al. 1995)

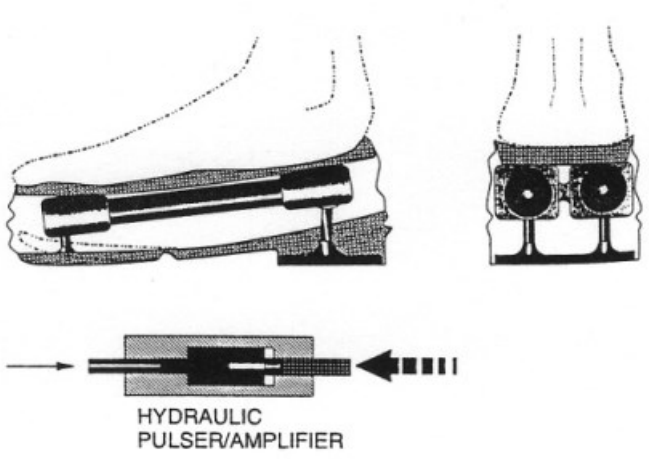

Figure 8. *Shoe energy harvester with hydraulic system. (Antaki et al. 1995)*

Although the power output is impressive, the shoe is rather obtrusive. For most of the energy harvesting shoes unobtrusiveness has been an essential design objective.

4.2 THUNDER-element and PVDF stacks

Piezoelectric shoe energy harvesters have been developed in the MIT Media Laboratory by several researchers since late 90's. All of them are basically based on the same concept that was first presented by Kymissis *et al.* In their approach two different piezoelectric generators are used to capture the energy from the bending of the sole and from the heel strike. (Kymissis et al. 1998)

To capture the energy from the bending of the sole 8 layers of 28 µm thick PVDF sheets are sandwiched on both sides of a 2 mm thick flexible plastic substrate as shown in Figure 9. All 16 PVDF layers are connected in parallel. When the stack is bent a voltage is created through the "3-1" longitudinal mode of piezoelectric coupling. (Kymissis et al. 1998)

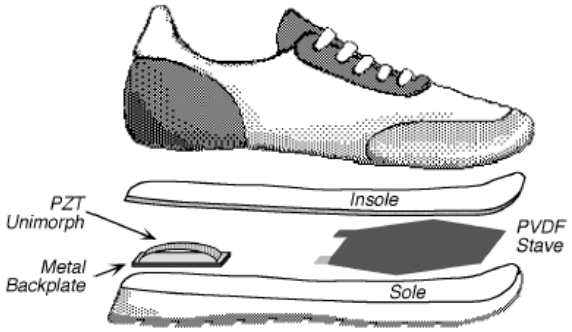

Figure 9. *Shoe energy harvester using a PVDF stack and a THUNDER –element. (Kymissis et al. 1998)*

To capture the energy from the heel strike a THUNDER (Thin Layer UNimorph Ferroelectric DriVER and Sensor) TH-6R unimorph piezoelectric element is used. The element is made of a composite PZT bonded on a curved piece of spring steel. This configuration allows a large deformation of the piezoelectric material without breaking resulting in higher energy yield. (Kymissis et al. 1998)

As approximate optimal resistances, 250 kΩ resistors were used for both elements. The elements were connected to the resistors through a rectifier and the voltage over the resistor was measured. At roughly 1 Hz frequency the energy output was about 1 mJ/step for the PVDF element and 2 mJ/step for the TH-6R element. The elements were used to power a RF Tag system. (Kymissis et al. 1998)

Kendall was researching the same design in his thesis reporting maximum average powers of 0,6 mW for PVDF stave and 5 mW for PZT with excitation frequency of 2 Hz. (Kendall 1998)

The concept was further developed by Shenck. He combined two THUNDER TH-6R elements in a configuration called dimorph, shown in Figure 10, to capture the energy

from the heel strike more efficiently. He reported a 8,4 mW power output with a 500kΩ resistor with 0,91 Hz frequency. (Shenck 1999)

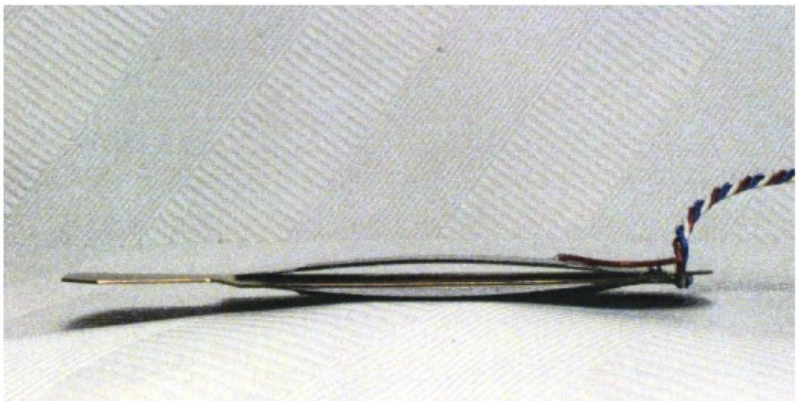

Figure 10 *The dimorph configuration. (Shenck 1999)*

Shenck and Paradiso did further research on an energy harvester using the dimorph and a PVDF stave to power a RF tag system. They reported average powers of 1,1 mW with the PVDF stave connected to a 250 kΩ load and 8,4 mW with the dimoprh connected to a 500 kΩ load at 0,91 Hz. Full bridge rectifiers were used in for both elements. When powering the RF tag system through forward converter a continuous power of 1,3 mW was achieved. (Shenck and Paradiso 2001)

Also Wang further researched this concept. He was experimenting, developing and optimizing electromechanical structures and investigating and implementing a series-SSHI circuit. At first he was investigating four piezoelectric elements: PVDF, THUNDER PZT, PZT ceramic stacks and MFC-PZT but in the end he discarded PZT ceramic stacks and MFC-PZT due to severe problems. (Wang 2010)

The structure of the PVDF stack Wang was developing is shown in Figure 11. He investigated the optimum width, length and placement for the PVDF sheets and the optimum number of PVDF layers in the stack as well as the adhesives and insole cores used in the stack. He found that the width can be as wide as needed but the length should be limited to the ball of the foot. He also found out that using the Delrin thin insole, that was used in previous studies, voltage cancellations occur because the bending of different layers does not happen completely uniformly. He then tested different insole cores. He determined the optimal number of PVDF layers to be three on both sides of the insole core in order to have a level of stiffness that was still comfortable for the user but provides a good energy generation. With the final PVDF stack configuration he achieved 4,93 mW power into a 4,167 MΩ resistor with a full bridge rectifier. (Wang 2010)

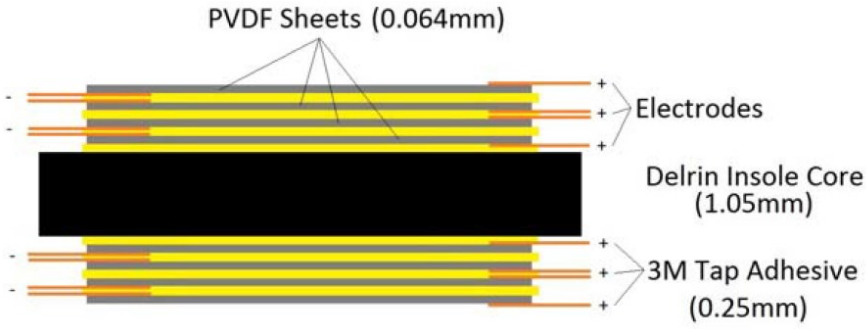

Figure 11. *Schematics of a 8-layer PVDF stack with Delrin insole core. (Wang 2010)*

To harness the energy from the heel strikes two THUNDER TH-6R's were used in a reversed clamshell design that is shown in Figure 12. With optimal load resistance of 1,48 MΩ, maximum power extracted with a full bridge rectifier was 5,94 mW. With series-SSHI rectifier a combined output of 11-13 mW was achieved. (Wang 2010)

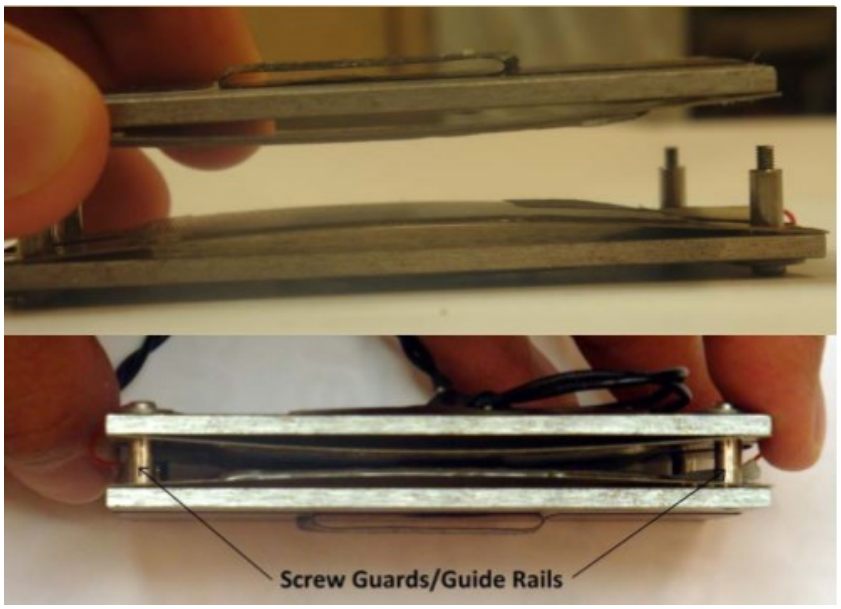

Figure 12. *The reversed clamshell design. (Wang 2010)*

4.3 Vertical PVDF unimorphs

Fourie developed a prototype of a shoe energy harvester using unimorph strips that were placed vertically in the heel of the shoe. The harvester is shown in Figure 13. A horseshoe-shaped piece of rubber material was cut from the heel of a sneaker and two polycarbonate plates were glued on the top and on the bottom of the piece. Shallow grooves were cut in the polycarbonate plates and fifteen elongated, rectangular unimoph strips were glued to these grooves. The unimorphs were made from PVDF and were connected in parallel to two copper terminals. (Fourie 2010)

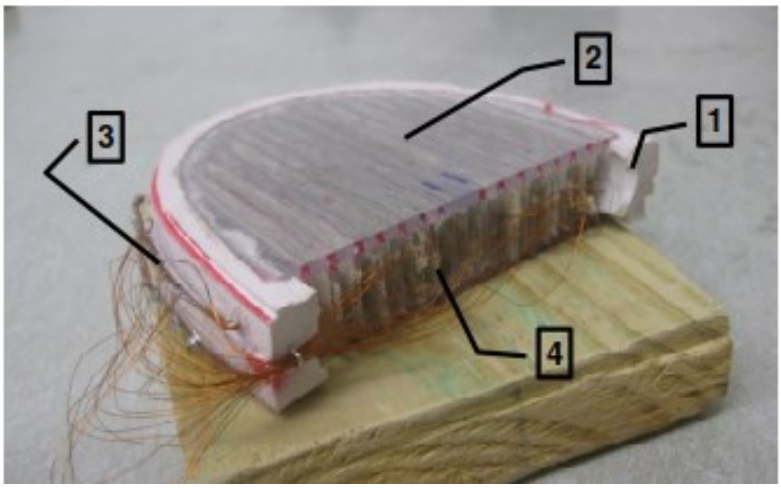

Figure 13. *Shoe insert composed of (1) a rubber cutout, (2) polycarbonate plates, (3) copper terminals, and (4) unimorph strips. (Fourie 2010)*

The raw output was determined by connecting resistors directly to the piezoelectric element. The optimum resistance was found to be 470 kΩ. At 1 Hz frequency the average power was 0,06 mW and when the piezoelectric element was connected with a full bridge rectifier to 1 μC capacitor the average power to the capacitor was 0,05 mW. (Fourie 2010)

4.4 Cantilevers

Mateu and Moll studied the optimal bending beam, i.e. cantilever, structure for energy harvesting shoes. They analyzed several structures suitable for the intended shoe inserts and the walking type excitation. The structures differed by dimensions, employed materials, and type of supports. The bending beam structure is used to convert the applied force from direction 3 to direction 1. The schematics of the cantilever inside the shoe is shown in Figure 14. (Mateu and Moll 2005)

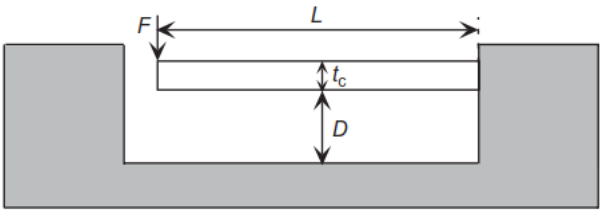

Figure 14. *Schematics of a bending beam in a shoe insole. L is the beam length, t_c is thickness and D is the cavity depth. (Mateu and Moll 2005)*

The power was calculated by terminating the electrodes with a resistor. Based on mathematical calculations they concluded that the most efficient support is a simply supported beam with a distributed load and the most efficient vertical structure is an asymmetric heterogeneous bimorph structure. The cavity depth is also a factor to consider. In general the bigger the cavity the better the output. (Mateu and Moll 2005)

Moro and Benasciutti were studying cantilever type energy harvesters for shoes. They presented a numerical and an analytical model of the energy harvester and also tested a

prototype that uses rectangular bimorph bending beam with PZT-5A layers. The harvester is shown in Figure 15. The piezoelectric element was connected to a test resistance of 14 kΩ (that was not optimized) to test the power output. The harvested power was approximately 13 µW. They discussed the effect of different parameters to the output and suggested improvements to the system concluding that outputs in the range of 293-395 µW can be achieved. (Moro and Benasciutti 2010, Benasciutti and Moro 2013)

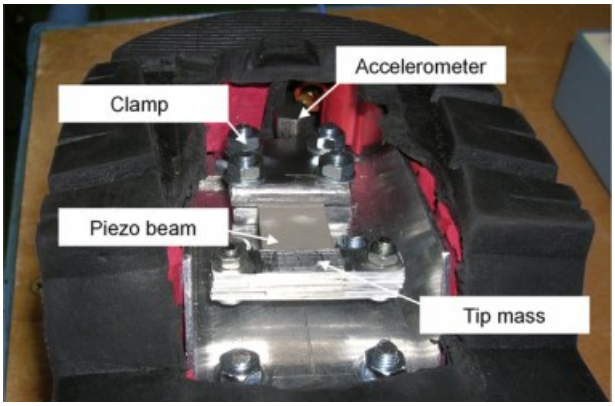

Figure 15. *Piezoelectric cantilever inserted in a shoe. (Benasciutti and Moro 2013)*

Camilloni *et al.* used a cantilever type piezoelectric element (MIDE Volture V22BL) to build the energy harvester shown in Figure 16. The cantilever was a piezoelectric composite beam with a proof mass attached to the tip of the beam. The harvested energy was used to power a system consisting of sensors, a microcontroller, and a wireless transceiver. The harvester provides an average output power of 75µW to the system during "fast speed" run. (Camilloni et al. 2016)

Figure 16. *Cantilever type energy harvester attached to a shoe. (Camilloni et al. 2016)*

Meier *et al.* developed an energy harvester from off-the-shelf elements to power a device that measures the foot pressure from six locations. The energy harvester is shown in Figure 17. It uses two piezoelectric elements, a rigid cantilever type element (Mide Volture – PZT) for the heel and a flexible element (Physik Instrumente Durract) for the ball of the foot. The cantilever was placed in a 3D printed enclosure where it can vibrate freely after a step. The flexible energy harvester was placed in the ball of the foot where the maximum bending occurs. An integrated circuit LTC-3588-1 was used for the rectification and an acrylic capacitor was used as the energy storage. Despite high

variability in operating amplitude and frequency an average energy of 10 − 20 μJ was captured per step. (Meier et al. 2014)

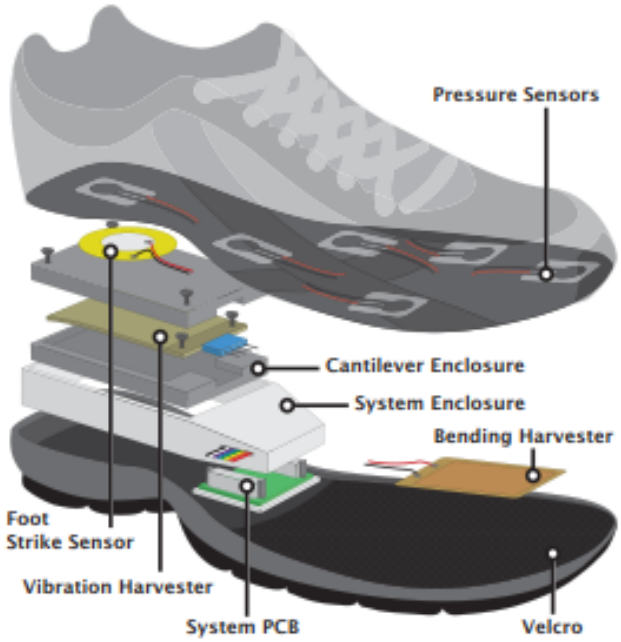

Figure 17. *Shoe energy harvester with a cantilever and a flexible piezoelectric element. (Meier et al. 2014)*

4.5 Piezoelectric cantilever with ferromagnetic ball

Fan *et al*. developed a shoe energy harvester that exploits the energy from vibrations, swing movement, and compressive force. The harvester consists of a piezoelectric cantilever beam magnetically coupled to a ferromagnetic ball and a crossbeam. The system is shown in Figures 18 and 19. (Fan et al. 2017)

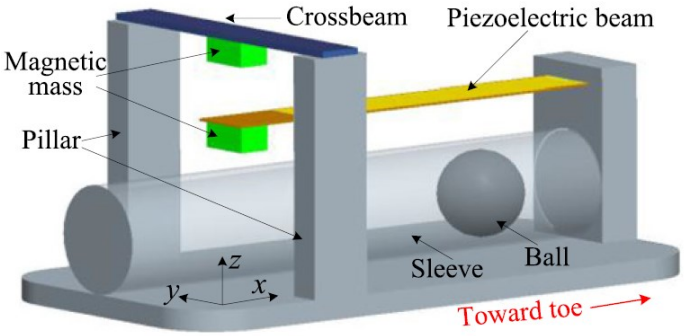

Figure 18. *Schematics of the shoe energy harvester using the magnetic coupling. (Fan et al. 2017)*

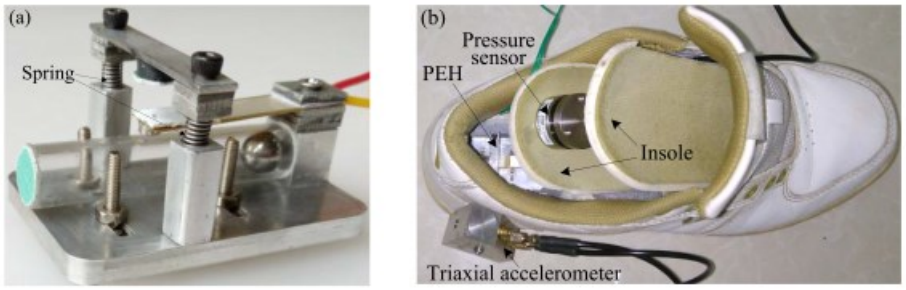

Figure 19. *Shoe energy harvester using the magnetic coupling a) harvester b) harvester inserted to a shoe. (Fan et al. 2017)*

The beam is designed to capture the vertical acceleration produced by a heel strike. During the heel strike the beam bends down and when shoe is lifted it bends up. The swing motion of the leg is captured by the ferromagnetic ball that travels along the sleeve (horizontal-axis) and triggers the piezoelectric beam to vibrate through magnetic coupling. The piezoelectric cantilever beam was made of a brass substrate and a piezoelectric patch. The output power generated by the fabricated prototype ranged from 0,03 to 0,35 mW when the walking velocity varied from 2 km/h to 8 km/h. (Fan et al. 2017)

4.6 PVDF films

Rocha *et al.* developed a shoe harvester made of PVDF film placed under the ball of the foot and under the heel as shown in Figure 20. They used a full bridge rectifier made of Schottky diodes and stored the energy in a thin film rechargeable lithium battery. They reported varying results depending on the area, the placement, the geometry, and the numbers of foils. The energy generated in one hour by a person applying four steps per second, when the harvester was connected to a 200 kΩ resistor, was at maximum 0,05 J. This translates into power of 13,89 μW. (Rocha et al. 2010)

Figure 20. *PVDF films attached to the shoe. (Rocha et al. 2010)*

4.7 PVDF films, buzzers and piezoelectric stacks

Gatto and Frontoni investigated four approaches to harvest energy from walking. The first approach used a PVDF film in a designed mounting. The second uses four piezoelectric buzzer elements under the heel and a PVDF film in the ball of the foot. The third solution uses 8 PVDF films on both sides of a harmonic steel. The fourth solution is a combination of a piezoelectric stack in the heel inside a 3D-printed mounting and a folded sheet of piezoelectric material in the ball of the foot. These configurations are shown in the Figure 21. (Gatto and Frontoni 2014)

Figure 21. *Four shoe energy harvester configurations. (Gatto and Frontoni 2014)*

4.8 PVDF rolls

Ishida *et al.* developed an energy harvester that uses PVDF rolls under the shoe as shown in Figure 22. 21 PVDF rolls are connected in parallel to a shared rectifier. When the rolls were pressed simultaneously the output voltage was maximized. When they were pressed non-simultaneously the voltages cancelled each other causing lower output. To avoid this, using multiple rectifiers in different areas of the shoe was suggested. They achieved a maximum power of 12 µW with 65 % power efficiency. (Ishida et al. 2013)

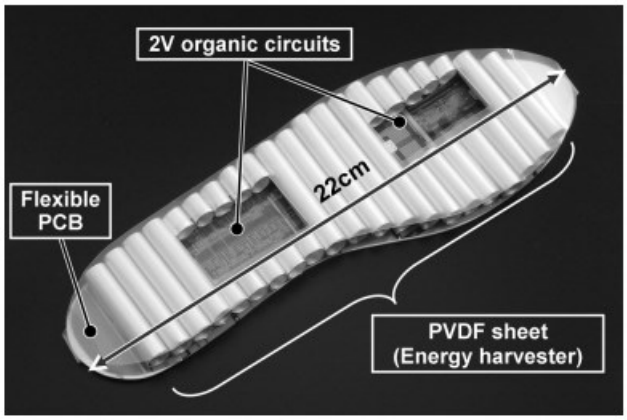

Figure 22. *Shoe energy harvester with PVDF rolls. The cut-outs are made to show the circuits behind. (Ishida et al. 2013)*

4.9 Multilayered PVDF between wavy surfaces

Zhao and You developed an energy harvester based on a multilayer PVDF film placed between two wavy surfaces. The concept is illustrated in Figures 23a and 23b. The PVDF film is attached to the bottom surface and the layers are connected in parallel. When a person is stepping on the harvester, the upper plate moves down stretching the layers as shown in Figure 23b. During step up the PVDF film returns to the original shape. During the deformation a voltage is created in the element. (Zhao and You 2014)

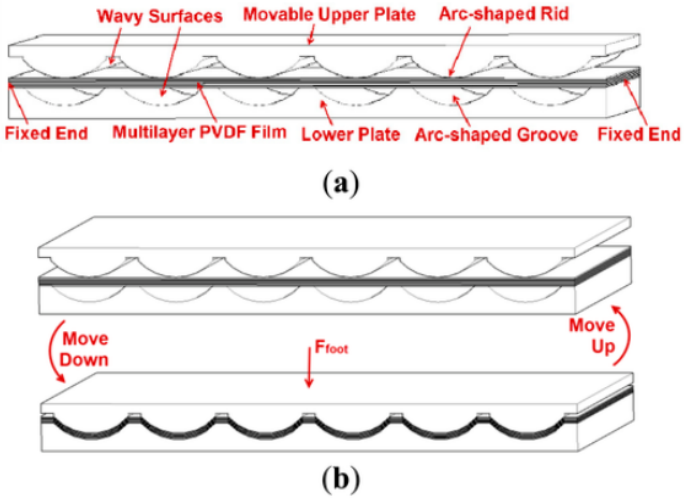

Figure 23. *A multilayer PVDF film between two wavy surfaces. a) Step up b) step down. (Zhao and You 2014)*

Two prototypes were made. In the first prototype an 8-layer PVDF structure with upper and lower plates made of engineering plastics is placed under the heel. In the second prototype first 8-layer PVDF structure was placed in the heel area and second in the ball of the foot as shown in Figures 24a and 24b. The upper and lower plates are made of silicon rubber that has lower stiffness compared with engineering plastics. The middle space was used for electronics. (Zhao and You 2014)

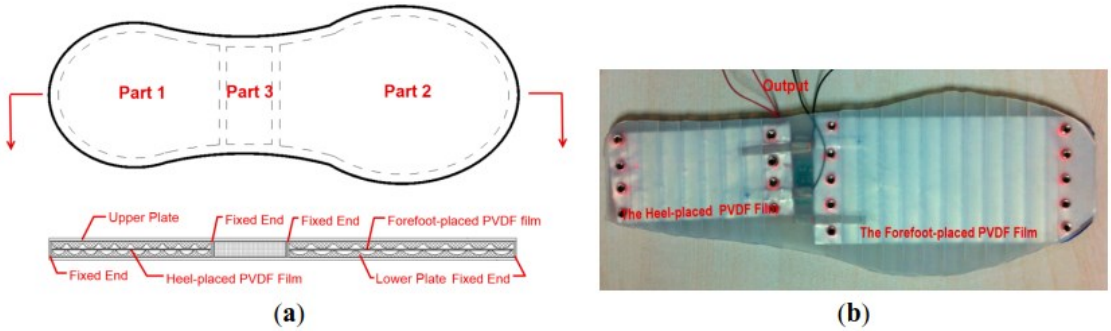

Figure 24. *a) Schematics of the prototype 2, b) prototype 2 implemented in the insole. (Zhao and You 2014)*

The prototypes were placed in the insoles, as shown in Figures 25a and 25b, and tested during a walk at 1 Hz frequency. When the prototype 1 was terminated with a 1,268 MΩ

resistor, the average power was 1 mW. In the prototype 2, the heel-placed PVDF film was terminated with a 1,682 MΩ resistor and the PVDF film in the ball of the foot with a 660 kΩ resistor. The average power for the heel was 30 µW and for the ball of the foot 90 µW, in total 0,12 mW. (Zhao and You 2014)

Figure 25. *Energy harvester a) prototype 1, b) prototype 2. (Zhao and You 2014)*

4.10 Roller support

Wischke and Woias developed an energy harvester that is made of low cost commercially available components, and that is easily implantable into the heel of a shoe. This approach was chosen because the shoe power generators presented before were considered too complicated and expensive. The main component is a PZT piezoelectric diaphragm (see Figure 26a) that is mounted on a roller support as shown in Figure 26b. (Wischke and Woias 2007)

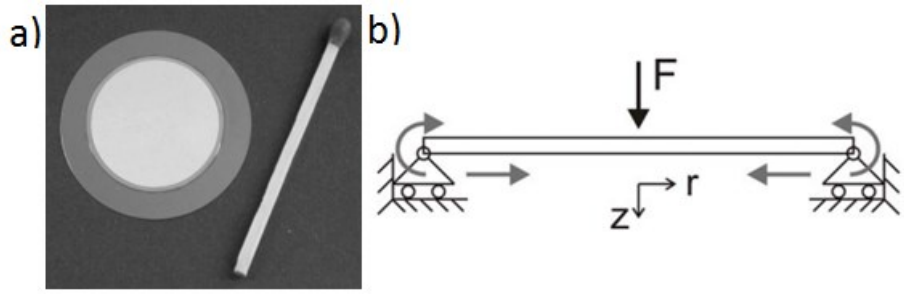

Figure 26. *a) Piezoelectric diaphragm, b) schematics of the roller support. (Wischke and Woias 2007)*

The maximum power with an optimal resistance of about 100 kΩ was 1,3 mW at 1 Hz with 10 N force using the three layer structure. The generators capability to charge a 1000 µF capacitor was also determined using a passive full bridge rectifier. (Wischke and Woias 2007)

4.11 Drum energy harvester

A drum transducer was developed by (Wang et al. 2007) and further investigated by Mishra *et al.* Mishra *et al.* developed a drum transducer for vibration energy harvesting (Mishra et al. 2015) followed by a study in which they developed energy harvesting shoes using drum transducers elements made of piezoelectric buzzers. The construction of the

drum transducers is shown in Figure 27. Two buzzers are attached back-to-back with a steel string. A drum stack is made by stacking individual drums. (Mishra et al. 2017)

Figure 27. *Schematics of the drum transducer. (Mishra et al. 2017)*

The elements placed in a shoe are shown in Figure 28. Rubber discs were adhered to the elements to couple the force to the active material and to provide restoring force. (Mishra et al. 2017)

Figure 28. *Drum transducers mounted in a shoe. (Mishra et al. 2017)*

Two models were made. Model 1 made of drum stacks and model 2 made of individual drums were tested with three different circuits: the standard interface circuit consisting of a bridge rectifier from Schottky SR100 diodes, a capacitor and a variable resistive load, circuit using MOSFET bridge rectifier and finally using LTC 3588-2. The maximum average powers for model 1 were 3,86 µW with the standard interface and 1,23 µW with the MOSFET rectifier. For model 2 the maximum average powers were 3,21 µW with the standard interface and 0,38 µW with the MOSFET rectifier. (Mishra et al. 2017)

4.12 Cymbal energy harvester

Palosaari *et al.* developed an energy harvesting system using a cymbal type piezoelectric transducer mounted in a shoe insole. The cymbal harvester was before studied in (Kim et al. 2004; Kim et al. 2006; Ren et al. 2010). The energy harvester designed by Palosaari *et al.* was made from PZT-5H piezoelectric disc, two brass rings for electrical connections and two convex steel plates that stretched the piezoelectric disc in "3-1" direction. The parts of the energy harvester are shown in Figure 29a and the assembled harvester in Figure 29b. The schematics of the harvester is shown in Figure 29c. Different variations

of steel plate thicknesses were tested. The energy harvester mounted in a shoe is shown in Figure 30. (Palosaari et al. 2012)

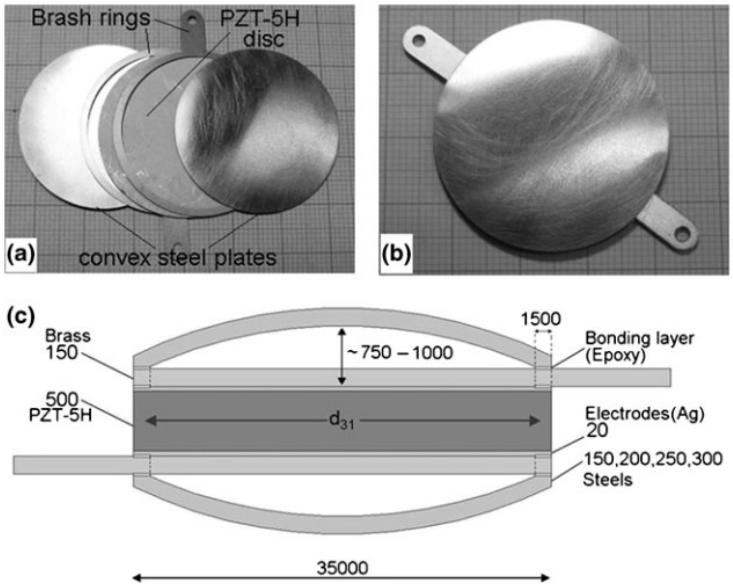

Figure 29. *The cymbal energy harvester. a) Parts of the harvester, b) assembled harvester, c) schematics of the cymbal harvester. (Palosaari et al. 2012)*

Figure 30. *The cymbal energy harvester inserted in a shoe. (Palosaari et al. 2012)*

Palosaari *et al.* found that the power generation is proportional to the ratio of piezoelectric layer's and steel plate's thicknesses, the frequency and the compression force. When the frequency was 1,19 Hz and force 24,8 N, the 250 µm steel plate generated the highest energy. When the piezoelectric element was connected directly to the approximate optimal resistance the average power was 0,66 mW. (Palosaari et al. 2012)

4.13 Diaphragm with pre-stress mechanism

Later Palosaari *et al.* developed an energy harvester based on piezoelectric circular diaphragm with mechanically induced pre-stress. The harvester was made from piezoelectric ceramic disc glued on a steel plate that was placed on clamping rings. The rings could adjust the height and the pre-stress of the disc with 16 screws. The pre-stress was made with a linear spring. Different parts of the energy harvester is shown in Figure 31a and the schematics of the harvester are shown in Figure 31b. (Palosaari et al. 2014)

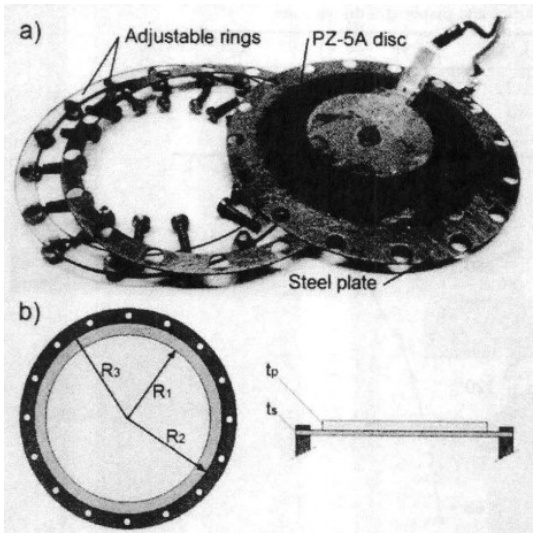

Figure 31. *Energy harvester using diahpragm and the pre-stress mechanism. (Palosaari et al. 2014)*

The bending caused by the pre-stress was varied from 0 to +0,6 mm and the bending due to compressions measured from non-prestress state from 0 to -1,1 mm. When the piezoelectric element was directly connected to the resistor, average maximum powers of about 1,1 mW was measured with frequency of 0,96 Hz and compression cycles of 1,5 mm. The energy harvesting capability improved over 141% with the pre-stress mechanism. (Palosaari et al. 2014)

This type of harvester was further developed by Leinonen *et al.* They were experimenting with stacking of these elements and testing them in walking and running tests. With four elements connected in parallel and terminated directly through a 147 kΩ resistor, maximum average power of 11,30 mW was measured at 1,07 Hz frequency. The power density was 10,55 mW/cm^3. The schematics of the harvester are shown in Figure 32 and the harvester fitted in a running shoe is shown in Figure 33. (Leinonen et al. 2016)

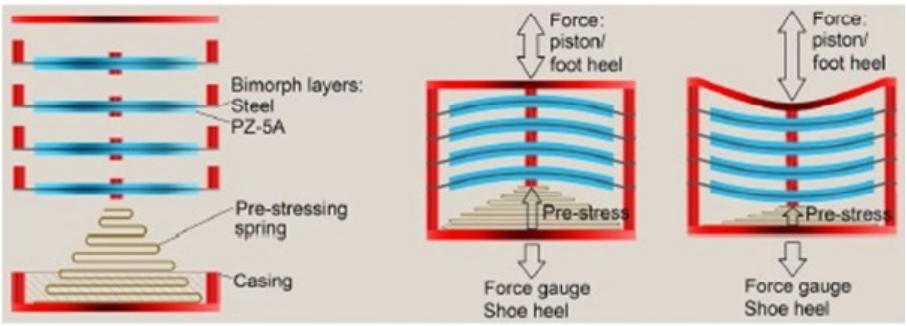

Figure 32. *Schematics of stacked diaphragms with the pre-stress mechanism. (Leinonen et al. 2016)*

Figure 33. *Stacked diaphragms with the pre-stress mechanism placed in a shoe. (Leinonen et al. 2016)*

Energy harvesting from walking with the cymbal energy harvester and with the energy harvester that uses diaphragms with mechanically induced pre-stress are also discussed in Palosaari's doctoral dissertation. (Palosaari 2017)

4.14 Sandwiched piezoelectric transducer

Kuang *et al.* developed a sandwiched piezoelectric harvester that was based to the cymbal type energy harvester design. The harvester uses a rectangular PZT plate sandwiched between two metal substrates and end caps that transfer the compressive force into tensile force and act as a force amplifier. The structure is shown in Figure 34. When the piezoelectric element was directly connected to an optimal resistance of 2 MΩ, the average power in a treadmill test was measured to be 2,5 mW with walking speed of 4,8 km/h. (Kuang Yang et al. 2017)

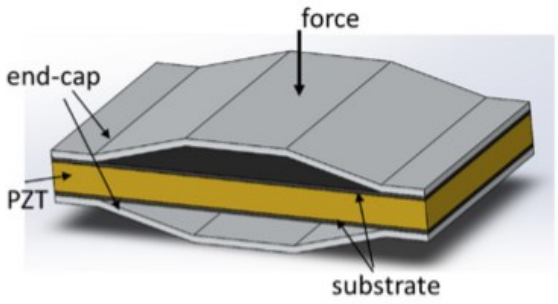

Figure 34. *Sandwiched piezoelectric transducer. (Kuang Yang et al. 2017)*

4.15 Rotary system

Howells developed a piezoelectric energy harvester that is made of four PZT-5A bimorph stacks that are deformed by a rotary cam. The linear motion of a step is converted into rotation of the cam with a lead screw and a gear train that deflects the stacks. The schematics of the harvester are shown in Figure 35a and the harvester in Figure 35b. A power electronics circuit converts AC to DC and stores the energy into a storage capacitor that powers a DC-DC converter that supplies 12V output pulses. On average the system produced 90,3 mW of power per compression. (Howells 2009)

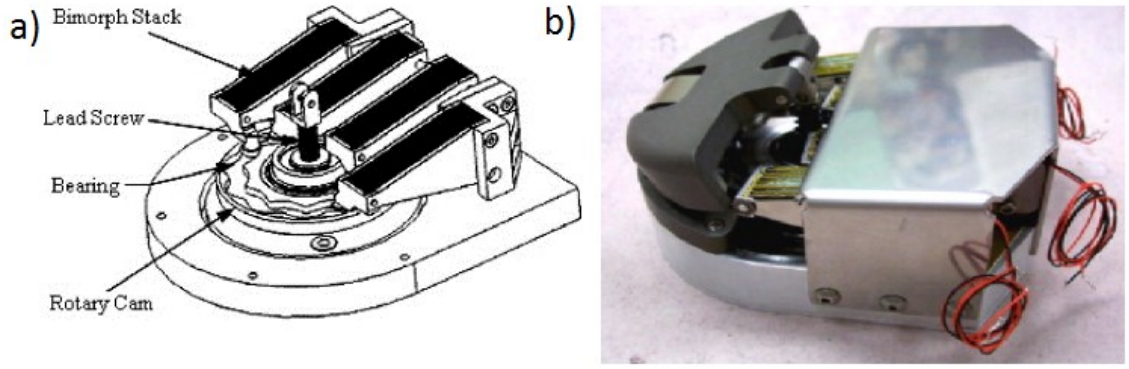

Figure 35. *a) Schematics of the rotary system, b) energy harvester with rotary system. (Howells 2009)*

4.16 Summary of shoe energy harvesters

The power generation capabilities of different shoe energy harvesters are gathered to the Table 2. The outputs are not directly comparable because the operating conditions (for example, usually authors have not taken into account such factors as weight of the user) and the energy harvesting circuits can be different. However, they can give an idea of the power levels that can be achieved with different configurations. The outputs are measured using the optimal resistance, except in the energy harvesters using cantilevers and PVDF rolls.

Table 2. *Energy harvester types and their power/energy outputs.*

ENERGY HARVESTER CONFIGURATION	POWER/ ENERGY	RECTIFIER	FREQUENCY	YEAR	AUTHOR
Hydraulic system	256-676 mW	full bridge	walking	1995	Antaki *et al*
PVDF (16 sheets)	1 mJ/step	full bridge	-	1998	Kymissis *et al*
TH-6R unimorph	2 mJ/step	full bridge	-		
PVDF (16 sheets)	0,6 mW	simple rectifier	2 Hz	1998	Kendall
TH-6R unimorph	5 mW	simple rectifier	2 Hz		
PVDF (16 sheets)	1,3 mW	full bridge	0,9 Hz	2001	Shenck & Paradiso
TH-6R dimorph (clamshell)	8,4 mW	full bridge	0,9 Hz		
PVDF (6 sheets)	4,93 mW	full bridge	1 Hz	2010	Wang
TH-6R dimorph (reverse clamshell)	5,94 mW	full bridge	1 Hz		
Combined	11-13 mW	full bridge	1 Hz		
Vertical PVDF unimorphs	0,06 mW	no rectification	1 Hz	2010	Fourie
Cantilever	13 µW	no rectification	1 Hz	2010 and 2013	Moro & Benasciutti
Cantilever	75 µW	full bridge (LTC-3588-1)	fast speed run	2016	Camilloni *et al.*
Cantilever and Physik Instrumente Durract - Processed PZT for the ball of the foot	10-20 µJ/step	full bridge (LTC-3588-1)	-	2014	Meir *et. al*
Piezoelectric cantilever with ferromagnetic ball	0,03-0,35 mW	no rectification	walking (2-8 km/h)	2017	Fan *et al.*
PVDF films	13,89 µW	full bridge	2 Hz	2010	Rocha *et al.*
21 PVDF rolls	12 µW	pMOS full bridge	1 Hz	2013	Ishida *et al.*
Multilayered PVDF between wavy surfaces, prototype 1	1 mW	full bridge	1 Hz	2014	Zhao & You
Multilayered PVDF between wavy surfaces, prototype 2	0,12 mW	full bridge	1 Hz		
Roller support	1,3 mW	no rectification	1 Hz	2007	Wischke & Woias
Drum harvester (stacks)	3,86 µW	standard interface	2 Hz	2016	Mishra Ritendra *et al.*
Drum harvester (individual drums)	3,21 µW	standard interface	2 Hz		
Cymbal energy harvester	0,66 mW	full bridge	1,19 Hz,	2012	Palosaari *et al.*
Diaphragm with pre-stress	1,1 mW	no rectification	0,96 Hz,	2014	Palosaari *et al.*
Stacked diaphragms with pre-stress	11,30 mW	no rectification	1,07 Hz	2016	Leinonen *et al.*
Sandwiched piezoelectric transducer	2,5 mW	no rectification	walking (4,8 km/h)	2017	Kuang Yang *et al.*
Rotary system	90,3 mW/compression	zener diodes	-	2009	Howells

5. ENERGY HARVESTER EXPERIMENTS AND DEVELOPMENT

In this section, the experimental procedure and the results as well as the developed energy harvester design are presented. First, the optimal resistance is determined. Next, different configurations of piezoelectric elements are presented and their maximum raw powers are determined. After that, the effect of a load capacitance on the energy harvesting efficiency is tested. Finally, the harvester's capability to charge a supercapacitor is tested in a treadmill test.

The energy harvesting circuits that are tested consist of piezoelectric elements, full bridge rectifiers and a load. A full bridge rectifier was chosen for the rectification because it is simple to build and is widely used in energy harvesting research. With more elaborated rectifiers the power extraction would be much better but to design one is out of the scope of this research.

The piezoelectric elements were made from piezoelectric diaphragms (MCABT-455-RC, available from Farnell element14) shown in Figure 36. The diaphragms were numbered to make them distinguishable and the ones used in the essential experiments are referred to. The full bridge rectifiers were made from four 21DQ06 Schottky diodes. Various resistors and capacitors were used as the load.

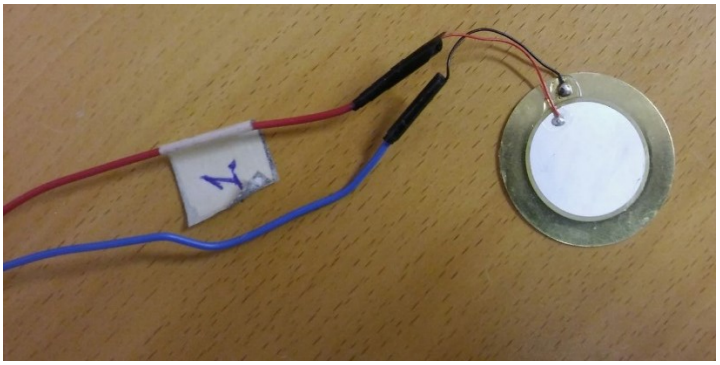

Figure 36. *Piezoelectric diaphragm.*

5.1 Optimal resistance

To be able to compare the developed energy harvester to the existing ones and to be able to evaluate the energy harvesting circuit losses, the optimal resistance and the corresponding maximum raw power are determined. To determine the maximum raw power, i.e. the power without rectification, the electrodes of a test piezoelectric diaphragm were terminated with various resistors ranging from 12 kΩ to 15,66 MΩ. The diaphragm was placed under the piston of a shaker (Bruel Kjær 4810 mini-shaker). A small static

force was applied to prevent the diaphragm from moving and a sinusoidal dynamic force with 1,25 N amplitude and 1 Hz frequency was applied. The diaphragm attached to the shaker is shown in Figure 37.

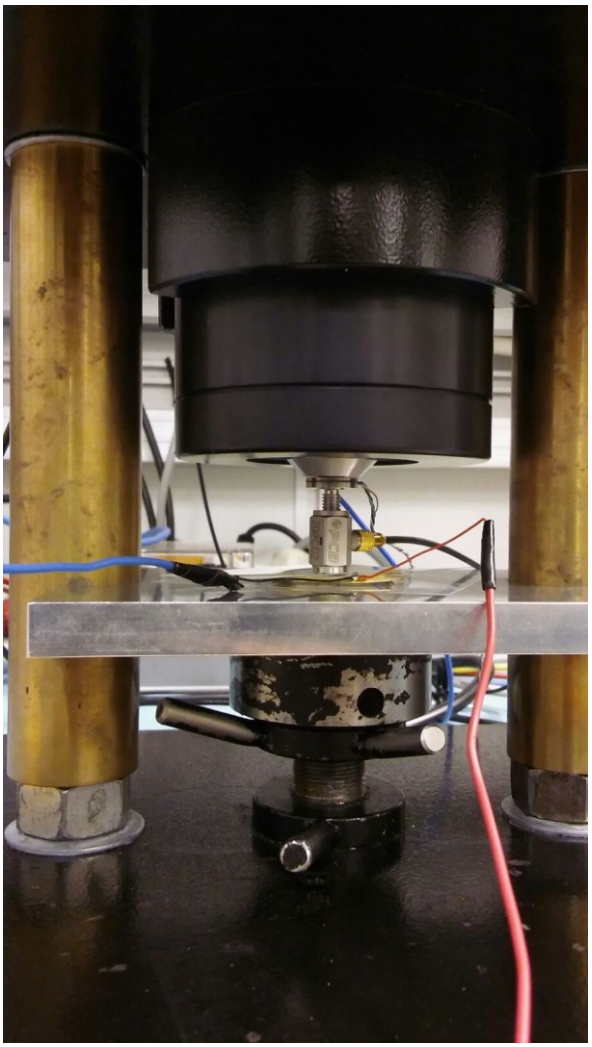

Figure 37. *The test diaphragm connected to the shaker.*

The voltage of the diaphragm was measured with a NI USB-4065 multimeter from National Instrument. The multimeter was able to take measurements approximately every 0,04-0,05 seconds. The maximum power of the diaphragm, in watts, was calculated from the maximum voltage for each resistor with the Equation

$$P = \frac{V^2}{R}, \tag{13}$$

and the 10 MΩ parallel resistance of the multimeter was taken into account in load flow analysis. The circuit is shown in Figure 38. The multimeter measured a sinusoidal response to the input force. Figure 39 shows the voltage over a 4,23 MΩ resistor. The maximum power dependence on the load resistor is shown in Figure 40. The optimal resistance is around 4 MΩ.

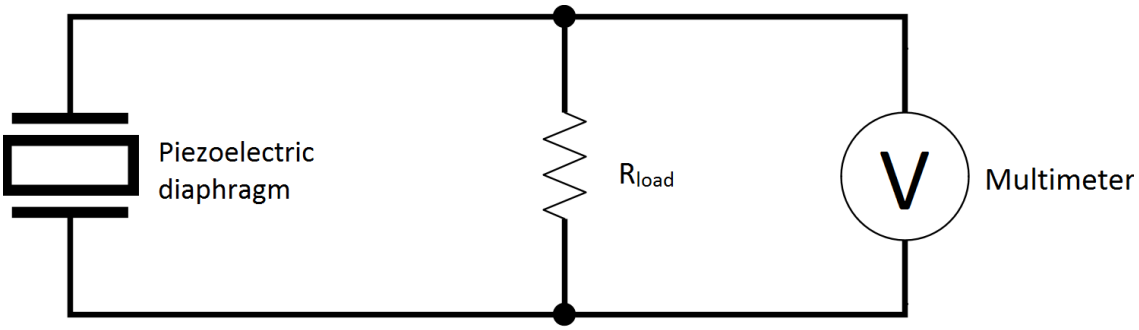

Figure 38. *Circuit used in defining the optimal resistance.*

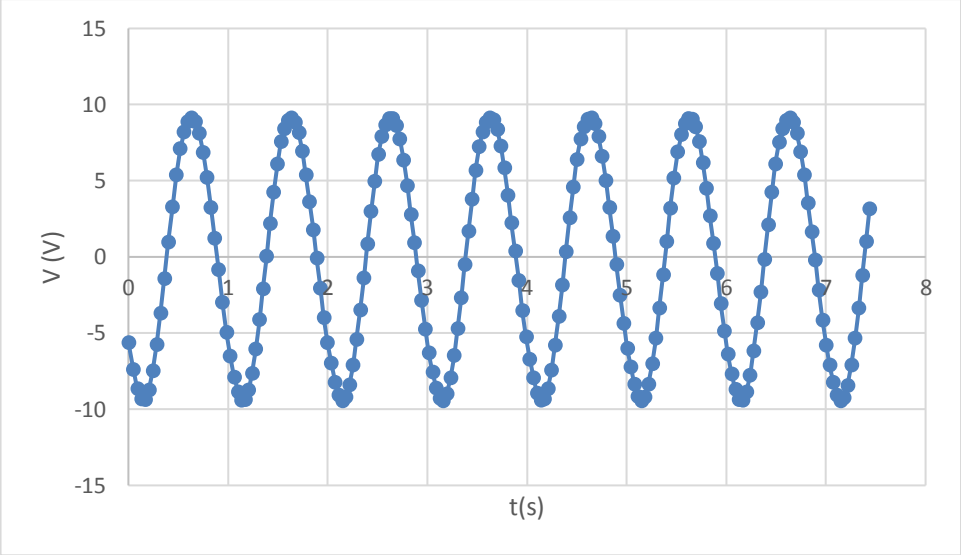

Figure 39. *Voltage of the diaphragm connected to the shaker and shorted with a 4,23 MΩ resistor.*

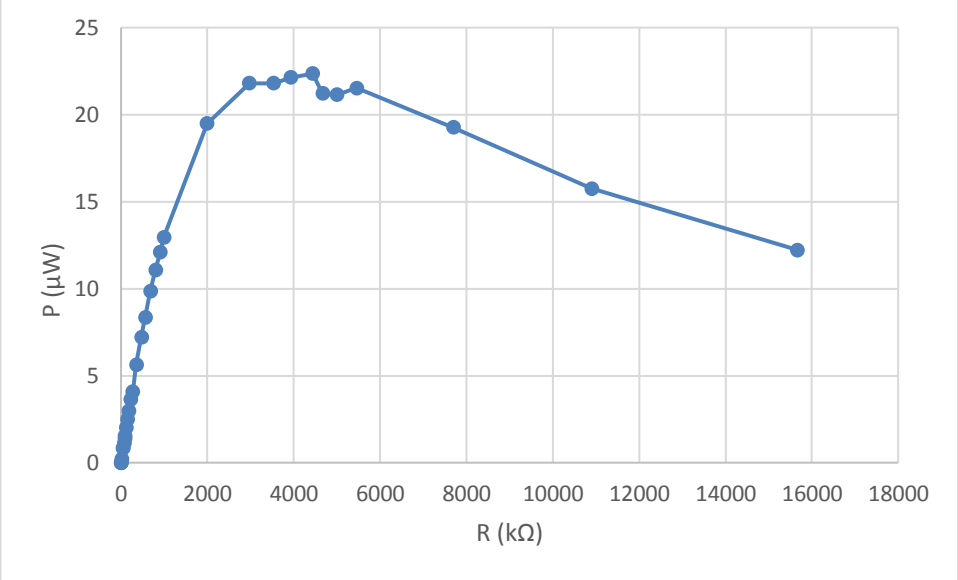

Figure 40. *Measured maximum power dependency on resistance*

5.2 Energy generations of different configurations

The energy generation capabilities of the diaphragms were then examined in step tests by measuring the amount of energy that is generated per step. All the tests were made by a test person weighting 65 kg and the stepping was tried to do as unaltered as possible. The piezoelectric elements were taped to the floor and the energy was calculated by using a known resistance and measuring its voltage with the multimeter. The instant power was calculated for all measurement points with the Equation 13. Then the energy in joules was calculated with the Equation

$$E = Pt\,, \tag{14}$$

multiplying the instant power by the time between the measured and the following measurement point to approximate the energy developed during this time. The energy generated during one step was then calculated by adding all the energies calculated between the measurement points during the step.

5.2.1 Flat diaphramgs

In preliminary tests it was noticed that the optimal resistance for energy generation in step tests was around 1 MΩ, not around 4 MΩ that was previously determined with the shaker, implying that the optimal resistance depends on the magnitude of the force. The raw power of the diaphragms 11-16 were tested when they were shorted with a 1,023 MΩ resistor. The power output ranged from 0,119 to 0,180 mJ/step. A typical voltage output of the diaphragms is shown in Figure 41. The peak voltage was typically around 30 V but even 40 V was occasionally reached.

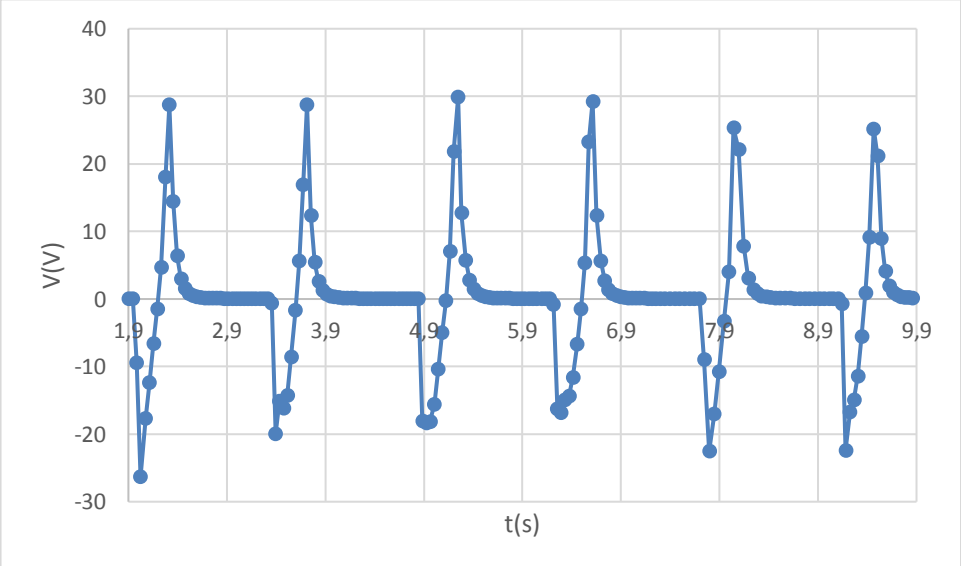

Figure 41. *Step test on flat diaphragm shorted with a 1,023 MΩ resistor.*

5.2.2 Diaphragm with beams

To increase the power output from the diaphragms 0,96 mm thick plastic beams were attached to the bottom of the diaphragms, as shown in Figure 42a, and a wooden beam was placed on top, as shown in Figure 42b, to allow the element to bend downwards from the middle. Because the piezoelectric diaphragms are very brittle they were protected with a piece of transparency and the beam thicknesses were limited to 0,96 mm. A typical output voltage of the configuration in step tests is shown in Figure 43. The peak voltages are around 100 V.

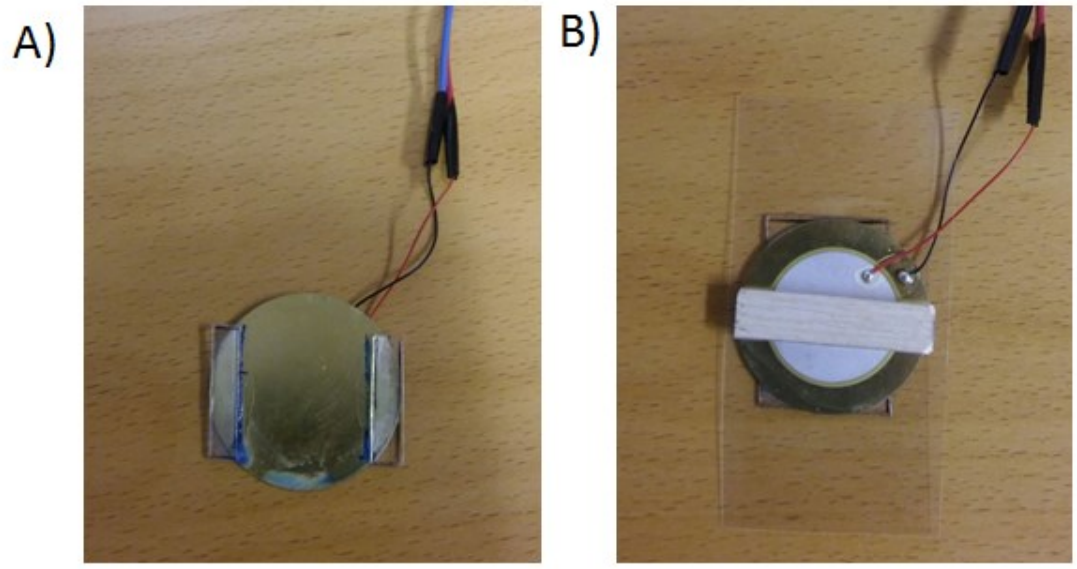

Figure 42. *The beams attached to the diaphragm. A) Bottom, B) top.*

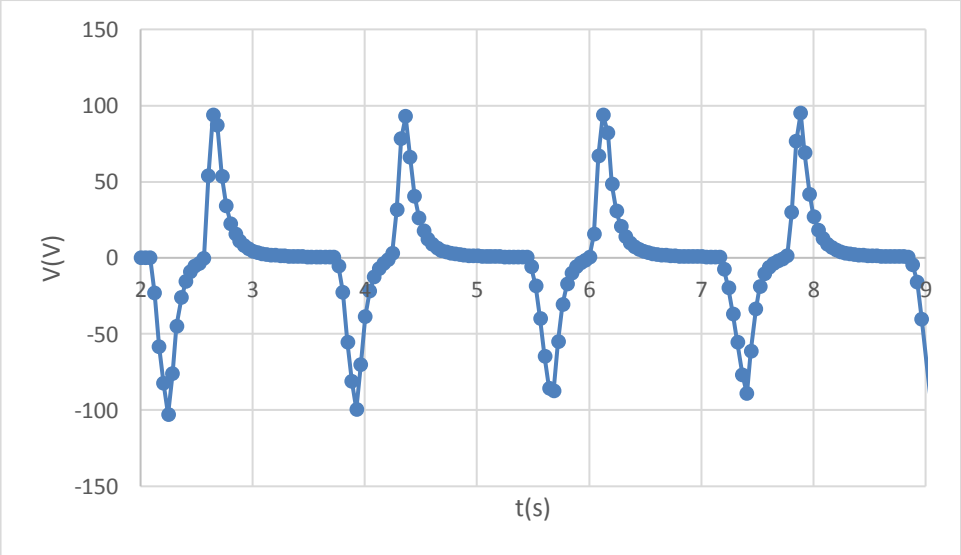

Figure 43. *Step test on the diaphragms with beams -configuration shorted with 1,023 MΩ resistor.*

The optimal resistance for this configuration was then validated. The results are shown in Figure 44 that shows that the highes energy is indeed generated with 1 MΩ resistance. When comparing the flat diaphragm with the diaphragm using the beams, the output was an order of magnitude higher. It was concluded that the bending should be exploited in the harvester design.

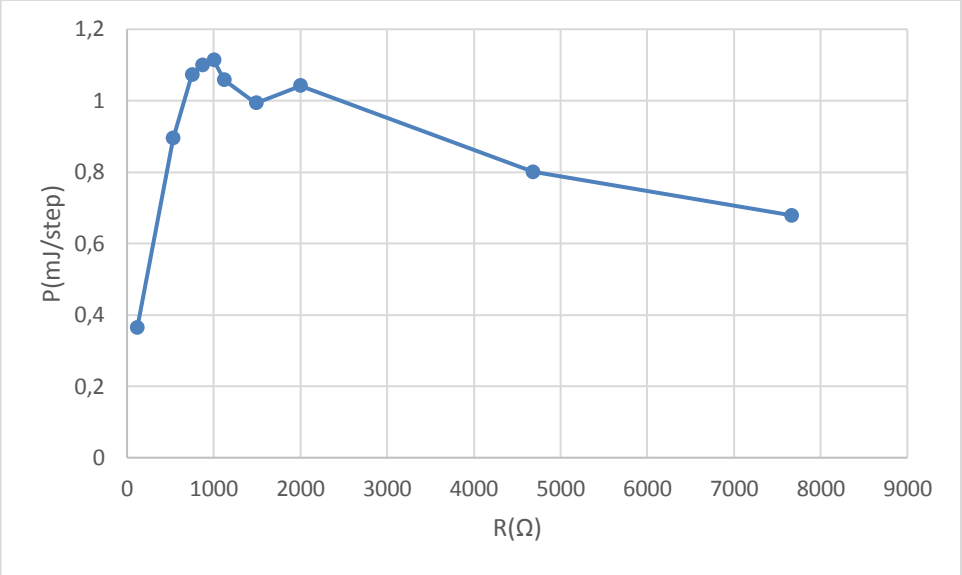

Figure 44. *Energy generation dependence on resistance for the diaphragm with beams –configuration.*

To evaluate the efficiency of the rectifier the average raw power and the average power with full bridge rectifier of elements 11-16 with beams were tested with a 1,023 MΩ resistor and the energy per step was calculated. The circuit diagram is shown in Figure 45 and the results are shown in Table 3. The energy extraction was about 27-41% lower when using the rectifier.

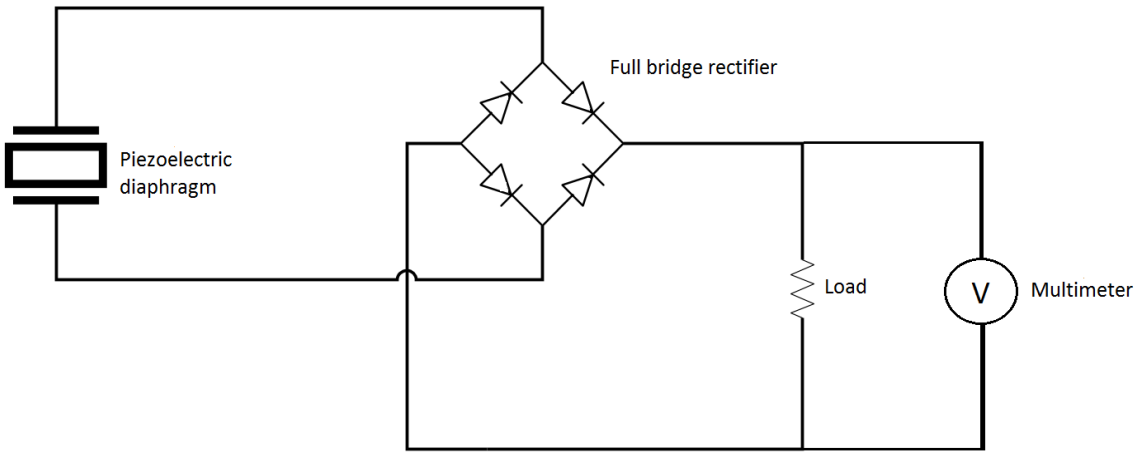

Figure 45. *Circuit diagram of the energy harvesting circuit with a full bridge rectifier.*

Table 3. *Diaphragms' raw powers without and with full bridge rectifier.*

Diaphragm	Raw power (mJ/step)	Rectified power (mJ/step)
11	1,508833	0,877948
12	1,075747	0,788765
13	1,189625	0,812482
15	1,113524	0,805839
16	1,248867	0,83321

5.2.3 Doubles

The diaphragms were then further examined in a combination that is referred as a "double" in this thesis. The configuration is shown in Figure 46. Two diaphragms with beams were placed between two stiff plastic plates that divide the force to the wooden beams and allow the diaphragms to bend down from the middle. Only elements with the same polarities were combined to prevent voltage cancellation.

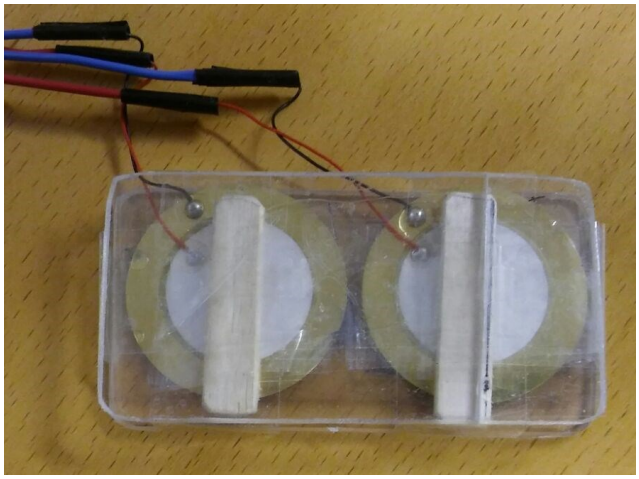

Figure 46. *Two diaphragms combines in a "double" configuration.*

The diaphragms 6 and 7, combined in a double (marked as {6,7}), were connected in parallel and in series to a shared rectifier and shorted with various resistors to test which arrangement would provide more power. The circuit for parallel connection is shown in Figure 47 and the test results are shown in Figures 48 and 49. Few resistances from both sides of the peak from Figure 44 was tested to compare the general power levels of parallel and series connections. The parallel connection was found to provide about 20 % more energy at maximum and was chosen as the arrangement for later tests.

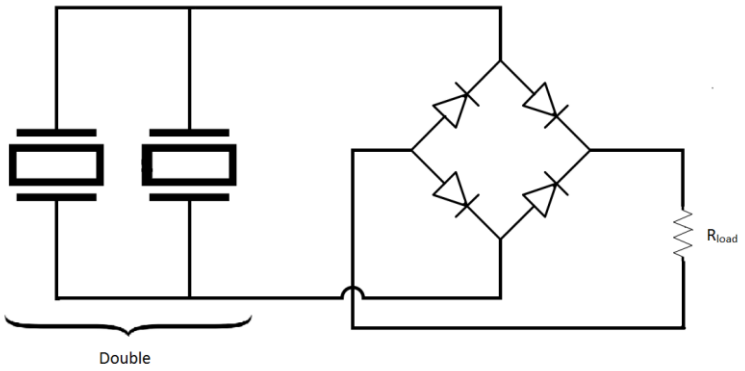

Figure 47. *Circuit diagram of the parallel connected double with shared rectifier.*

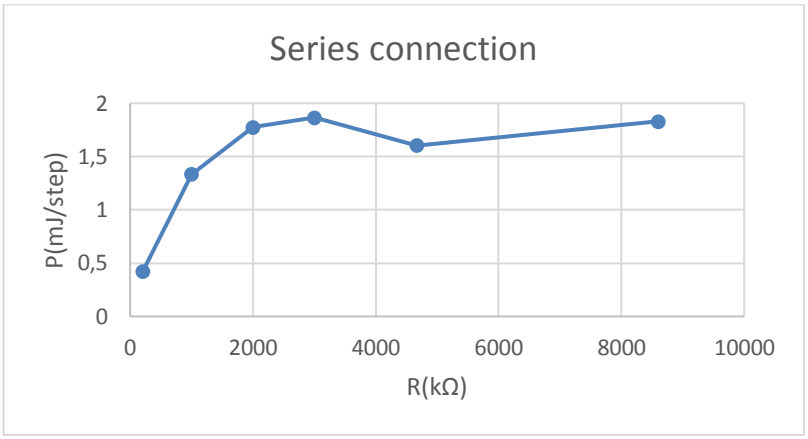

Figure 48. *Energy generation dependence on resistance for series connected diaphragms.*

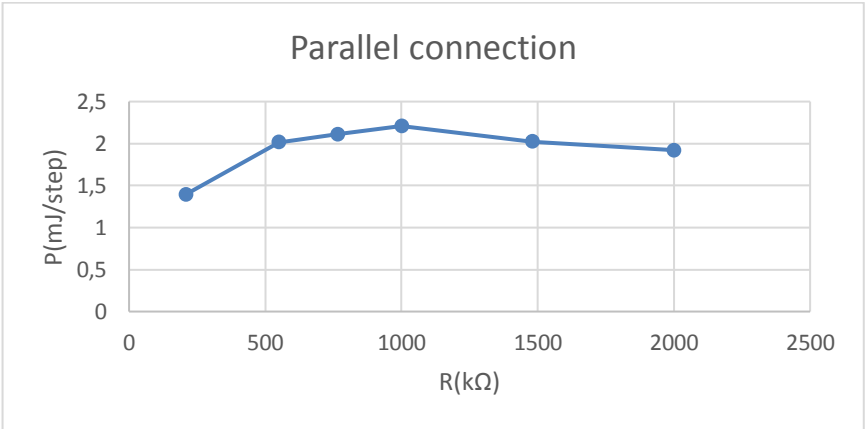

Figure 49. *Energy generation dependence on resistance for parallel connected diaphragms.*

Further tests were made to find out how much the rectifier limits the power extraction when using doubles instead of single diaphragms and whether each diaphragms should be connected with separate rectifiers or should shared rectifier be preferred. The test resistance was 1,023 MΩ. First the double {13,16} was tested using separate rectifiers for

both diaphragms and then using shared rectifier. The average output from several repetitions was calculated. With separate rectifiers the circuit produced 1,08 mJ/step and with shared rectifier 1,16 mJ/step. The higher output with shared rectifier might be due to lower overall turn-on losses in the diodes. Shared rectifiers were used in the following tests. The output of different doubles with shared rectifiers was then measured and compared with the outputs without rectification. The results are shown in Table 4. The rectified powers were about 36-50 % lower. Typical rectified voltage and current wave forms of the doubles are shown in Figure 50.

Table 4. *The energy generation of doubles with and without rectifier.*

Element	Raw power (mJ/step)	Rectified power (mJ/step)
{13,16}	2,306055	1,156999
{12,15}	2,136021	1,249774
{6,7}	2,208739	1,421523

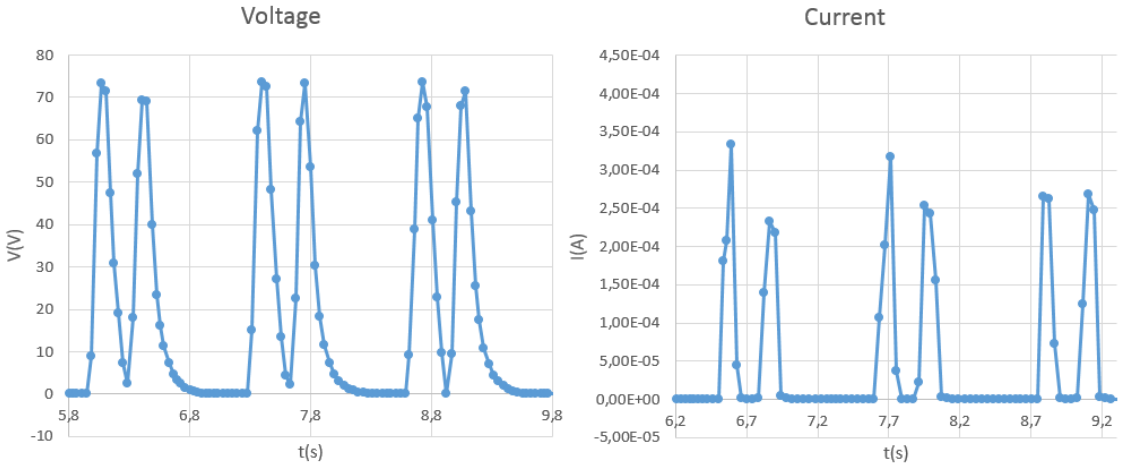

Figure 50. *Typical voltage and current wave forms of the doubles.*

Then the energy extraction using two doubles simultaneously was tested with the circuit shown in Figure 51. When the doubles {12,15} and {13,16} were piled on top of each other and connected to the resistor, the energy generated was 1,718 mJ/step. When they were placed next to each other on the floor and stepped simultaneously, the energy generated was 2,056 mJ/step. Calculating the separate rectified powers of {12,15} and {13,16} from table 4 together, the total power would be 2,407 mJ/step. The force on each double is less when they are stepped on simultaneously what limits the power extraction.

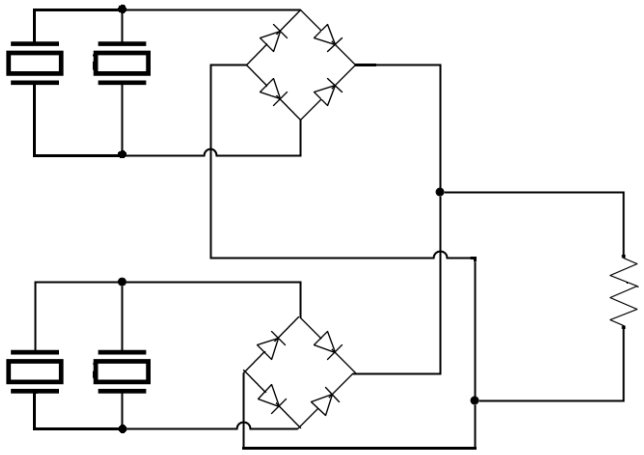

Figure 51. *Two doubles connected in parallel and shorted with a resistor.*

5.2.4 Shoe

Next the doubles {12,15} and {13,16} were placed inside a shoe. One was placed to the ball of the foot and one to the heel as shown in Figure 52.

Figure 52. *Two doubles inserted to a shoe.*

The breadboard was taped on top of the shoe and the voltage over the 1,023 MΩ was measured during walking. The output was fairly constant as can be seen in Figure 53. Figure 54 shows the voltage during one step. The first two peaks are the step down and the latter two peaks are the step up of the heel and the ball of the foot respectively. The average output from several test was about 1,764 mJ/step.

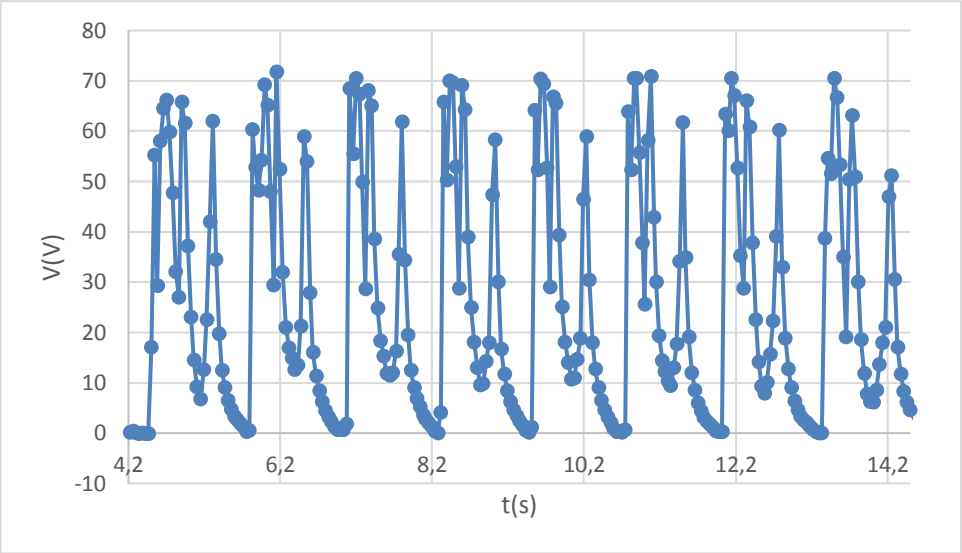

Figure 53. *Wave form of the doubles placed in the shoe during walk.*

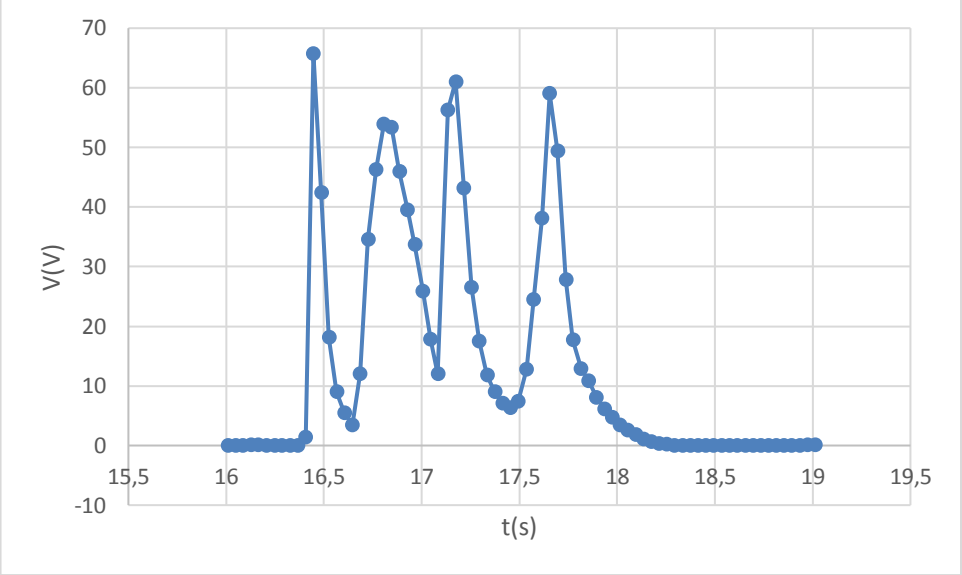

Figure 54. *Wave form of a single step.*

The output of the doubles {13,16} and {12,15} was again tested after the walking test in step tests separately using shared rectifiers. It was found out that the average output was a bit higher than earlier before the walking test: 1,292 mJ/step for the {13,16} and 1,321 mJ/step for the {12,15}.

5.3 Charging capacitors

The doubles' capability to charge capacitors was then tested. The circuit is the same as in Figure 47 except the resistor is replaced with a capacitor. Determining the energy stored to the capacitors per step was more challenging than expected since the capacitors seemed to leak quite fast. The smaller the capacitance was the faster the charge leaked. Figures 55 and 56 illustrate the discharging for 4,7 uF and 470 uF capacitors. The capacitors were

first charged up and then the discharging was observed by connecting the multimeter for short moments to measure the voltage at different times.

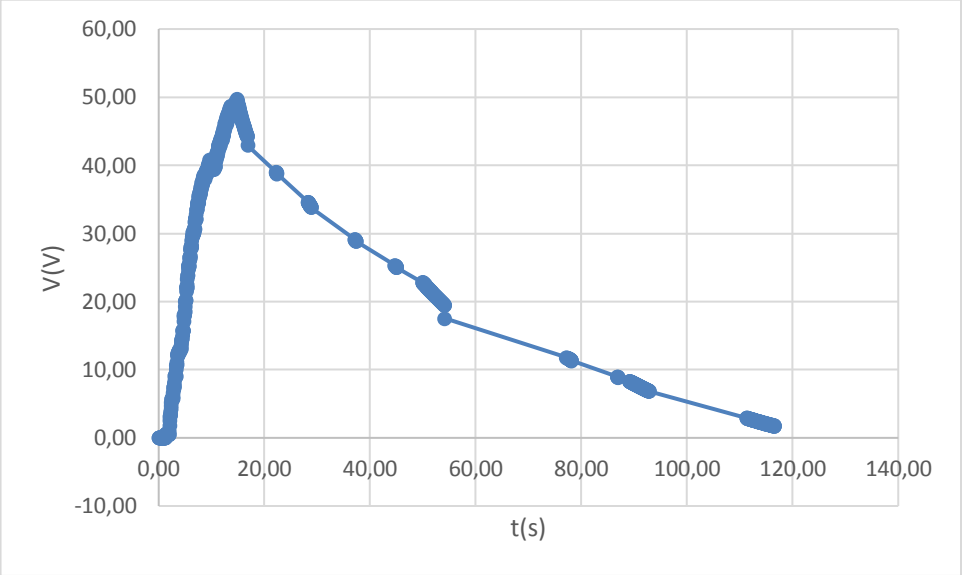

Figure 55. *Measurement of the leakage charge of a 4,7µF capacitor*

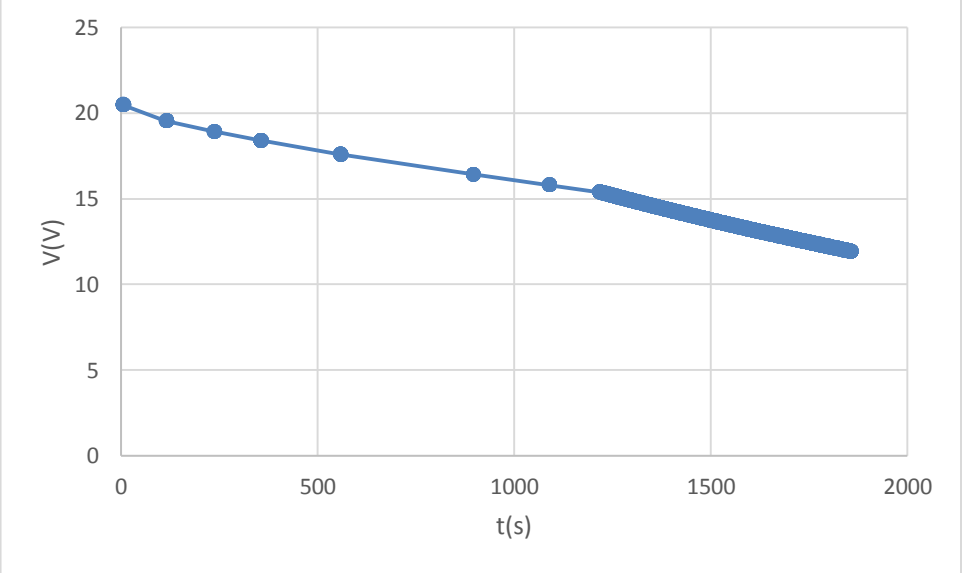

Figure 56. *Measurement of the leakage charge of a 470 µF capacitor. The multimeter stays connected from t=1220s.*

It was then decided to keep the multimeter connected continuously and measure the voltage created by single steps. As a result the capacitors charged up to specific voltage and then discharged as shown in Figure 57. The energy stored in the capacitors per step was calculated from the maximum voltage of the capacitor with the Equation

$$E = \frac{1}{2} C V^2 \ . \qquad (15)$$

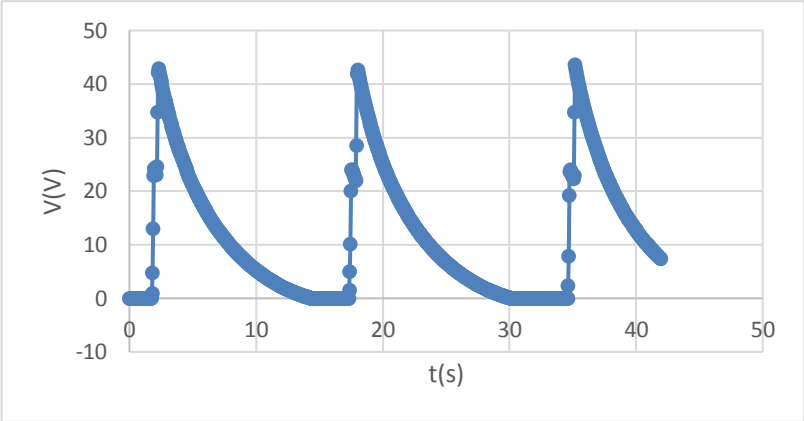

Figure 57. *Voltage of a 0,8 µF capacitor during steps.*

By this method it was found that the energy generated per step is highest with capacitor of 0,6 uF reaching about 0,8 mJ/step. With higher and lower capacitances, the energy generation decreases quickly both ways as shown in Figure 58 and 59. With 4,7 uF the energy is already only 0,2 mJ/step.

The peak voltage that was measured by connecting the multimeter straight to the outputs of the rectifier without any load is about 73,7 V. When decreasing the capacitance under 0,25 µF the voltage reaches its maximum twice during a single step as shown in Figure 60 and calculating the energy from the maximum voltage seems unlogical. This is why the 0,25 µF capacitor is the lowest capacitor taken into account in these Figures.

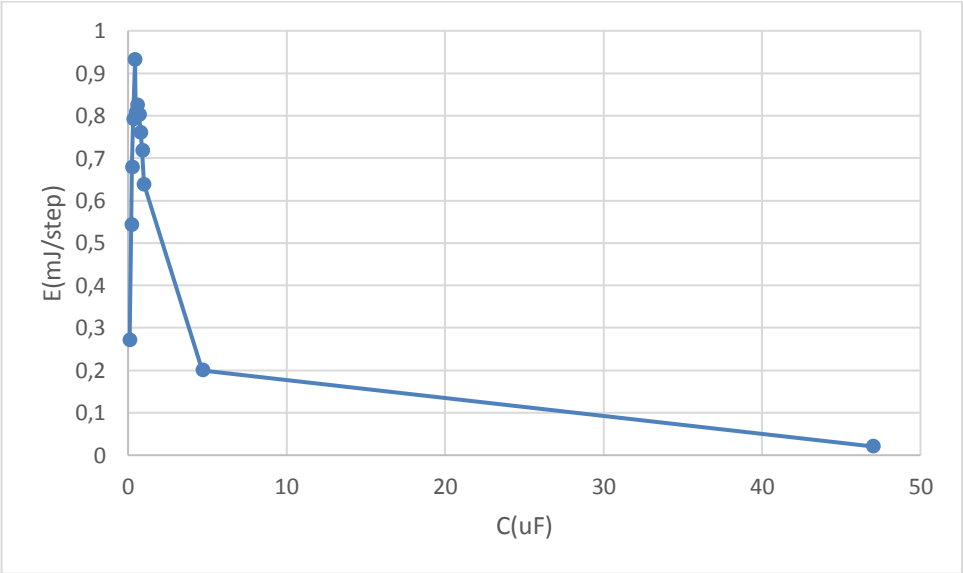

Figure 58. *Energy generation dependence on capacitance for single steps.*

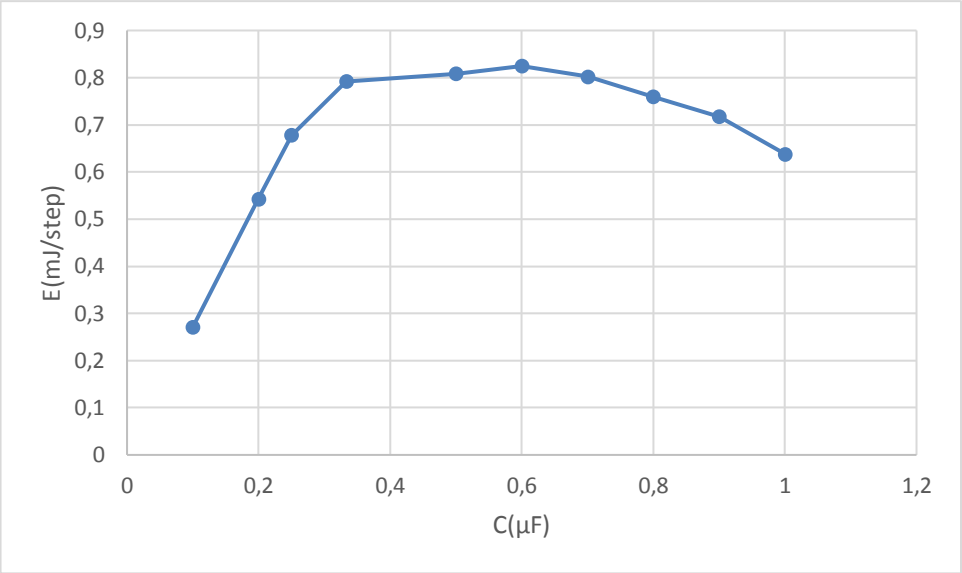

Figure 59. *Energy generation dependence on capacitance for single step; Zoom in to the peak.*

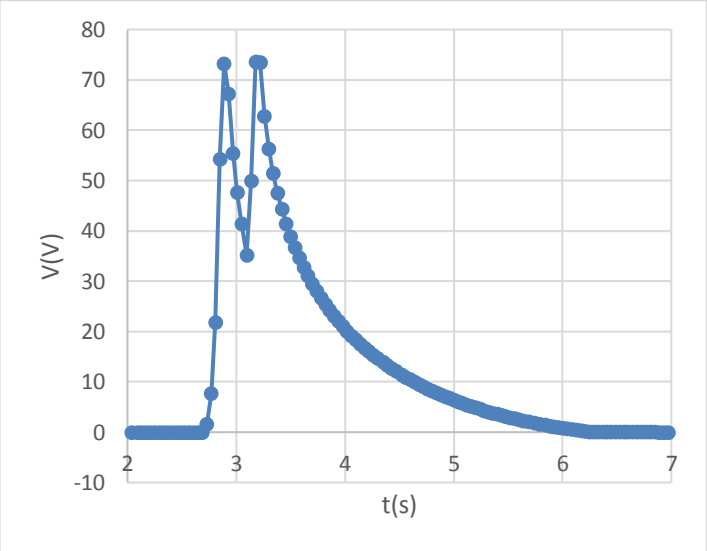

Figure 60. *Stepping on a 0,1µF capacitor.*

5.4 Treadmill test

Supercapacitor was chosen as the storage element in the treadmill test because they are with reason favored as energy storages in energy harvesting applications by some researcher as explained before. Furthermore, in the used energy harvesting circuit they did not show high leakage in contrary to the smaller capacitances with conventional capacitors.

The shoe energy harvester was made from two doubles that were inserted into a shoe as described before. The doubles were connected in parallel to a supercapacitor with 0,47 F capacitance. The circuit schematics are the same as shown in Figure 51 except the resistor is replaced with the supercapacitor. The shoe with the supercapacitor connected is shown in Figure 61. The energy harvester's capability to charge the capacitor was tested during a 20 minutes and a 30 minutes walk. The supercapacitor was discharged in the beginning and the multimeter was disconnected during the walk. After 20 minutes the multimeter was briefly connected to measure the voltage and then the walking was continued another 10 minutes. The frequency of the steps on the energy harvester was approximately 0,92 Hz.

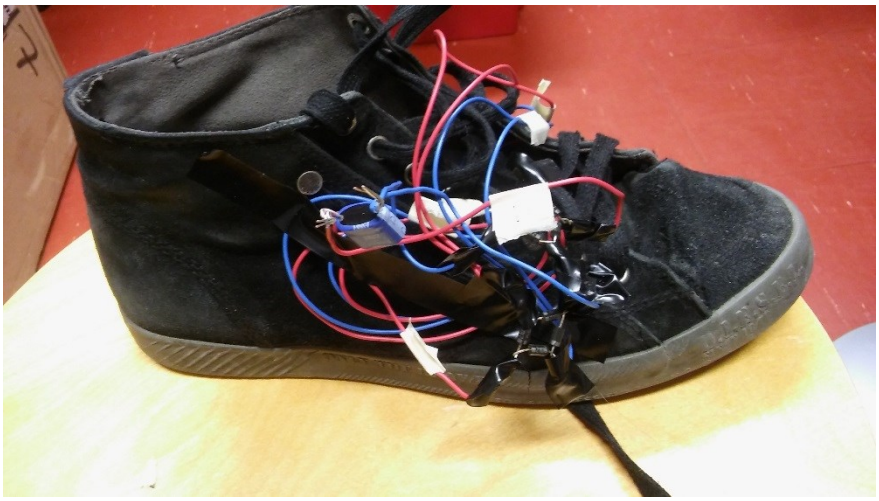

Figure 61. *Supercapacitor connected to the piezoelectric elements that are inserted in the shoe.*

Three different tests were made with the same configuration. In the final test with double {10,11} in front and {6,7} in the back, the supercapacitor was charged to 147,44 mV after 20 minutes walk and to 204,7 mV after 30 minutes. This translates into energies of 4,63 µJ/step and 5,95 µJ/step respectively. The leakage current was estimated by measuring the voltage of the capacitor connected to the energy harvesting circuit when 20 and 30 minutes had passed after the walking test. The voltage decreased 5,678 mV and 8,376 mV respectively.

Eventually in all tests, the double placed in the ball of the foot cracked. In the final test, the cracking happened around 220 seconds. After the walking test, the energy output of the shoe energy harvester was again tested using a 1023 kΩ resistor as the load. The measured output power stayed fairly constant around 1,13 mJ/step, although the output voltage form shown in Figure 62 was slightly different from the original form shown in Figure 53.

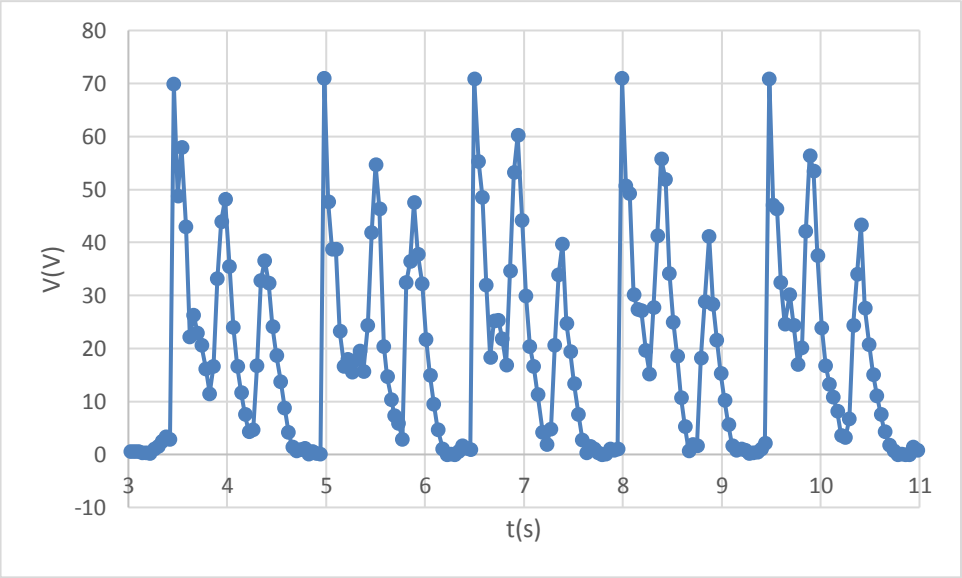

Figure 62. *Wafe form of the shoe energy harvester with a broken front-double.*

Figure 63 shows that the wooden beam of the right diaphragm has slipped from the middle of the front-double. Also the plastic plate on top cracked from the right side.

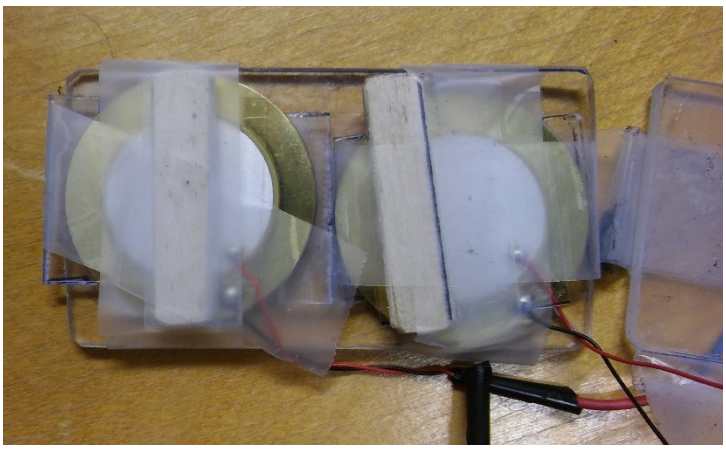

Figure 63. *Front-double after treadmill test.*

Figure 64 shows that also the left element suffered some damage although the wooden beam maintained its position after the plastic cracked.

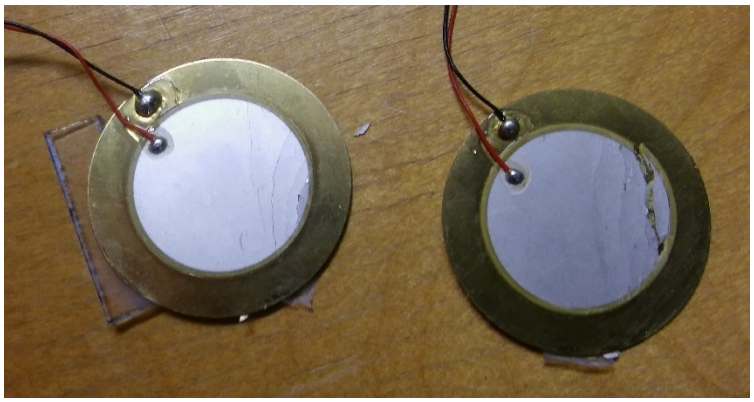

Figure 64. *Front-double dismantled.*

The double in the back, shown in Figure 65, did not suffer any visual damage during the tests.

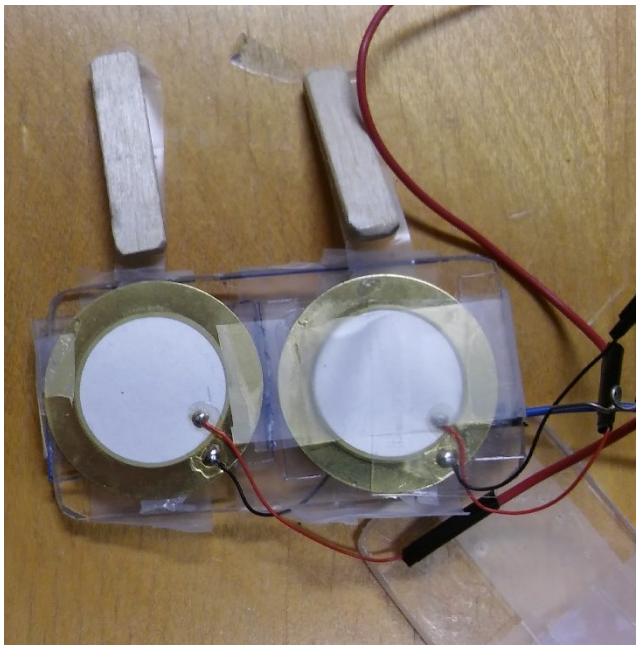

Figure 65. *Back-double dismantled.*

6. DISCUSSION

In this section, the results and possible applications for shoe energy harvesters are discussed.

6.1 Suggestions and observations from the measurements

There are several ways to improve the shoe energy harvester presented here both electrically and mechanically. Altogether it is quite bulky and uncomfortable to the user but it demonstrates successfully the feasibility of harvesting energy from walking. In more elaborated design the piezoelectric elements could be integrated into the shoe replacing some of the insole material. However, this might complicate the efficient mechanical coupling of the footstrikes. In any case, with a proper choice of materials and improved design the harvester should be made more durable to make it suitable for practical use.

In addition to the mechanical structure of the harvester, developing an efficient energy harvesting circuit is an essential. This issue was addressed in the experiments presented previously by finding optimal resistances to generate maximum raw powers with different configurations. For practical applications it is often important to be able to store the energy and therefore experiments were made to find the optimal capacitance for power extraction. Next, some observations from the experiments about the efficiency of the energy harvester are presented.

6.1.1 Optimal resistance

The optimal resistance for different configurations was determined to find the maximum power generation and to be able to compare the harvester with existing ones. Kim *et al.* approximated the optimal resistance of a piezoelectric energy harvester with Equation

$$Z = \frac{1}{2\pi f C_0}, \tag{16}$$

where f is the operating frequency and C_0 is the capacitance of PZT ceramic measured at a frequency of 100 Hz. (Kim et al. 2004) The data sheet of the piezoelectric diaphragm gives 37 nF ± 30% as the capacitance. If the capacitance is 37 nF then according to the Equation 16 the optimal resistance would be 4,3 MΩ which matches quite good with the measurement results when using the shaker with sinusoidal input force. In step tests, the optimal resistance was about 1 MΩ suggesting that with larger input forces the optimal resistance if different. To further improve the energy generation also factors such as the

size of the piezoelectric elements and the optimal bending without breaking should be investigated.

6.1.2 Series vs. parallel connections

When comparing the output from parallel and series connection of the piezoelectric diaphragms it was found that the parallel combination generates slightly more energy per step. As the current generated with energy harvesters is usually small, many researchers favor parallel connection because it allows the generation of larger current. The series connection allows generation of higher voltages but as the voltages are quite high also with the parallel connection, increasing the voltage is not desirable. Nevertheless, some studies have found series connection better. In Wang's energy harvesting circuit, the series connection of the piezoelectric elements yielded a 22% increase over the parallel connection (Wang 2010). This might be due to the particular energy harvesting circuit design.

6.1.3 Optimal capacitance

The energy harvesting efficiency measurements to different capacitors are questionable. According to the measurements, a 0,6 µF capacitor provided the best response considering the energy generated to the capacitor by a single step, and with lower and larger capacitances the energy of the capacitors decreased fast. This behavior might be explained with Equations 15 and 17. The energy stored in capacitor, E, can be defined with the equation

$$E = \frac{q^2}{2C}, \tag{17}$$

where q is the charge in capacitor. If the charge generated in the piezoelectric element is constant every step, depending on the element design and the stepping force, then according to Equation 17 the energy of the capacitor would get lower with increasing capacitance.

The energy stored in capacitor can also be defined with equation 15, shown in previous Chapter. With low capacitance, the maximum voltage generated by the piezoelectric element might limit the energy of the capacitor according to Equation 15. Also Fourie found that when using a 100 µC capacitor instead of a 1 µC, the stored energy is about an order of magnitude lower (Fourie 2010).

However, Roundy found in his studies with a similar circuit that the power transfer to the storage capacitor is the more efficient the larger storage capacitor is used. This is illustrated in Figure 66. He also found that the power transfer to a purely resistive load is

higher than to a capacitive load which was also validated by the measurements presented here. (Roundy 2003)

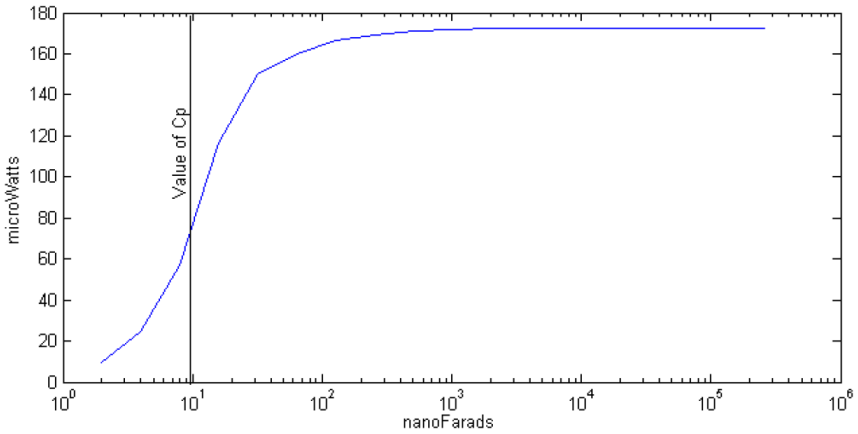

Figure 66. *Power transfer with different storage capacitances. (Roundy 2003)*

Either way, the design presented in this thesis managed to capture only a small fraction of the raw energy to the energy storage what suggests that the energy harvesting circuit is inefficient.

6.1.4 Improved efficiency during walk

In the treadmill test, it seemed that the energy captured per step was higher when calculated for 30 minutes compared with 20 minutes, although the double in the ball of the foot cracked after first few minutes. After cracking, it should produce less power. The higher power, when calculating for 30 minutes, might be due to the warming of the piezoelectric elements during the walk. An increase in the output of the doubles was also noticed in the step tests. The piezoelectric *d* constant of PZT typically increases with temperature (Li et al. 2009) which can improve the energy harvesting during walking. There might also occur pyroelectric effect but presumably in very low magnitude. This might also explain the increased energy output.

6.1.5 Degradation of piezoelectric materials

The degradations of the piezoelectric elements was not taken into account in the measurements because it would require longer term testing. For practical applications, this is a factor to consider. According to Platt *et al.,* it is well known that repeated mechanical and electrical cycling of PZT ceramics results in progressive degradation in performance as a function of time. The degradations depends on factors such as the amplitude, frequency, duration of applied mechanical and electrical loads, and the structure of the material. (Platt et al. 2005)

Platt *et al.* performed preliminary test on the degradation of a PZT stack with 440 N input force amplitude. During the first 10^4 cycles the degradation was neglible and after 20 million cycles less than 17 % of the initial value. The results can be seen in Figure 67.

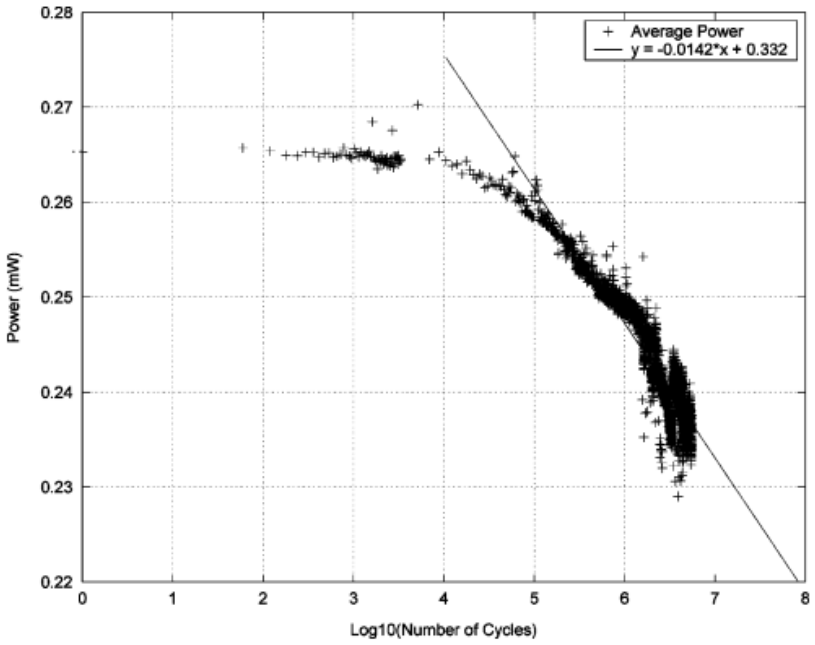

Figure 67. *Degradation of PZT stack. (Platt et al. 2005)*

The input force profile of a shoe energy harvester is different but if the degradation speed would be similar, the 17 % degradation would happen after 6,3 years of continuous walk at 1 Hz which could be acceptable considering the life time of the shoes.

Also Pillatsch *et al.* investigated the degradation of piezoelectric materials for energy harvesting and concluded that there is a need for broader scope of future research on this topic in order to guarantee the lifetimes of commercial applications. This will inspire confidence and widespread adoption. (Pillatsch et al. 2014)

6.2 Applications for shoe energy harvesters

The raw power output after rectification of the demonstrated shoe energy harvesters are 1,13 – 1,76 mW per step. Before rectification a single diaphragm generated around 1 mW with approximate optimal resistance. Therefore, with four diaphragms 4 mW/step raw power could be theoretically harvested. With 1,16 mW/step output with optimal resistance after rectification the energy harvester could charge the 0,47 F supercapacitor only 4,63 - 5,95 μJ/step. Most of the piezoelectric shoe energy harvesters have an output in the range of 1- 10 mW/step. Next I will discuss what to do with the harvested energy.

Charging mobile phones and other portable devices with shoe energy harvesters is an attractive idea and would be very useful form of power supply in remote areas. Several enthusiasts and researchers have been inspired by this idea and various types of shoe energy harvester designs that can supply power to phones via USB ports or with other

means have been developed. Paul *et al.* even proposed charging phones using piezoelectric generators and wireless power transfer (Paul et al. 2015).

Charging phones with a power supply between 1-10 mW seem rather impractical. For example, iPhones have battery capacity ratings in the range of 5,25 – 11,1 Wh (Apple 2018). With a power supply of 1 mW from piezoelectric shoe energy harvester it would take 5250 – 11100 hours to fully charge phone that is turned off. With 10 mW power it would be 10 times faster but it would still take more than 20 days of continuous walk to charge a phone.

With shoe energy harvesters, that use some other technology, charging phones seem more realistic. Shenck and Paradiso demonstrated a rotary generator that could provide average power of 250 mW (Shenck and Paradiso 2001) and some developers claim to have as high as 400 mW power generation capability with a shoe energy harvester that uses the mechanical energy of walking to spin a micro generator (Griffiths 2014). However, these solutions are rather obtrusive what is a major obstacle for widespread adaption. Some unobtrusive alternatives are based on dielectric elastomers (Wendt et al. 2012) or on moving liquid microdroplets (Hsu et al. 2015). Hsu *et al.* claim to be able to generate 1 W of usable power with a shoe energy harvester based on reverse electrowetting on dielectric with the fast self-oscillating process of bubble growth and collapse (Hsu et al. 2015). A company InStep NanoPower, LLC was based around this concept and they claim to have developed the first practical footwear embedded energy harvester. (Instep Nanopower n.d.).

Nevertheless, there are several applications that can be operated with the output of 1 mW generated with piezoelectric shoe energy harvesters. These are for instance various MEMS and wireless sensor nodes, and particularly wearable sensors. Wearable sensors can be used in various wireless health monitoring devices. Accorcing to Leonov most of these devices can work at a power less than 1 mW (Leonov 2011). According to Mitcheson *et al.* wireless sensors seems to be the primary application area for motion harvesters at least in the short range (Mitcheson et al. 2008). However, since the harvester is located in a shoe it would be quite complicated to deliver the power to other areas of body where most of the wearable sensors are.

Other than medical applications that could be powered with shoe energy harvesters could include personal tracking and recovery systems (Mitcheson et al. 2008), and calculators, watches, radios, and Bluetooth® headsets (Raju and Grazier 2010). Piezoelectric shoe energy harvesters have also been proposed as energy sources to replace batteries in various equipment worn by soldiers (Snehalika and Bhasker 2016) but the current power generation levels are not enough for most of the devices. Besides, it seems that there are better alternative power sources available for these devices. For example, the PowerWalk® Kinetic Energy Harvester, that is placed to the wearer's knees, can generate 10-12W while walking (Bionic Power n.d.). Furthermore, Palosaari suggested that shoe

energy harvester powered carbon monoxide detectors could be used to protect firefighters and workers from hazardous environments and that they could also power humidity and temperature sensors (Palosaari 2017).

A few applications powered by different kind of piezoelectric shoe energy harvesters have already been demonstrated. Kymissis *et al.* demonstrated an active RF tag that transmits a short-range wireless ID code to the vicinity while walking (Kymissis et al. 1998). This can be used in "active environment" systems that require the information about the locations of the users (Want et al. 1992). Camilloni *et al.* presented a device consisting of sensors (accelerometers), a microcontroller and a wireless transceiver. In a running competition they powered a LED with the energy harvester (Camilloni et al. 2016). Ishida *et al.* developed a shoe insole pedometer that also worked as a piezoelectric energy harvester (Ishida et al. 2013). Meier *et al.* demonstrated a shoe-mounted energy harvester for a system that measured the pressure of the wearer's foot on six locations (Meier et al. 2014).

The power from shoe energy harvesters can be accumulated to energy storages. This way the energy harvesters can power applications that do not work continuously but require higher power levels. To give an idea of the power consumptions of different devices and operations tables 5-8 are provided. Table 5 shows roughly the magnitudes of power requirements of some selected portable devices.

Table 5. *Power consumptions of portable devices. Adapted from (Leonov 2011, GNS-Electronics n.d., Palosaari 2017, Rocha et al. 2010, Vullers et al. 2009, Snehalika and Bhasker 2016, Bhatnagar and Owende 2015).*

Device	Energy consumption (mW)
Smartphone	
conversation	780
standby	42
MP3 Player	50-97
Low power GPS	
acquisition	72
tracking	25,2
backup	0,0252
Wireless sensor node	0,001-100
Mag Lite	19
Headset	19
Carbon monoxide detector	
alarm state	1,7
standby	0,0018
Hearing aid	1
Heart rate meter	0,83
Respiratory rate meter	0,83
Wearable EEG	0,8

Cardiac pacemaker	0,05
Quartz watch	0,005

Table 6 and 7 shows estimations of the power and energy consumptions in common wireless technology standards for different modes of operations

Table 6. *Power consumption of wireless transmission technologies. Adapted from (Choperena 2013).*

Power states (mW)	**Wi-fi**	**Zigbee**	**Bluetooth Low Energy**
Sleep	0,01	0,004	0,008
Receive	90	84	28,5
Transmit	350	72	26,5

Table 7. *Power consumption of wireless transmission technologies. Adapted from (Schlingloff 2014).*

Energy consumption during transmission	**Power (µW/bit)**
ANT	0,71
BLE	0,153
Wi-Fi	0,00525
ZigBee	185,9

Table 8 shows the power and energy consumptions of two common memory storages.

Table 8. *Idle power consumption and energy consumption of read and write operations of NAND-flash and SD-card. Adapted from (Carroll and Heiser 2010).*

Metric	**NAND-flash**	**SD-card**
Idle (mW)	0,4	1,4
Read (J/bit)	1,83E-09	3,85E-09
Write (J/bit)	1,19E-08	2,29E-08

Figure 68 sums up the power requirements for various devices and the energy harvesting capabilities from different sources.

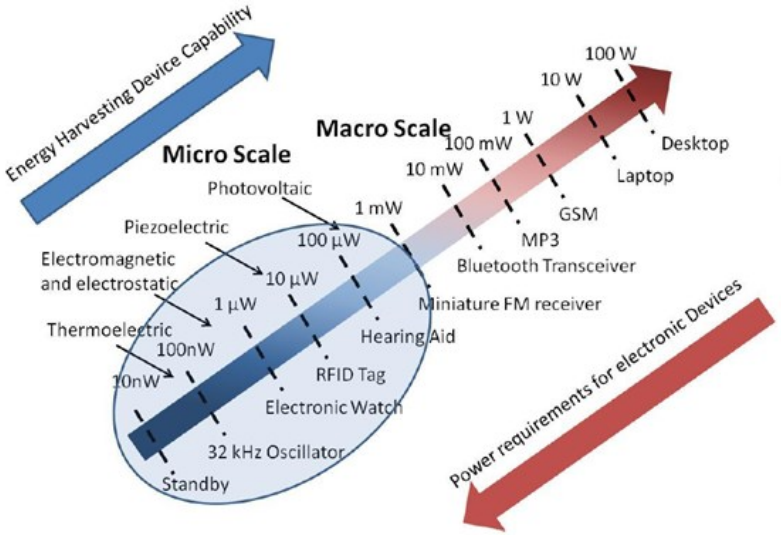

Figure 68. *Power requirements of various electronic devices and energy generation capability of different technologies. (Jackson n.d.)*

7. CONCLUSIONS

This thesis reviews the literature about various piezoelectric energy harvesters integrated into shoes. Most of the harvesters use some type of mechanism to bend the piezoelectric element whether the element is made from flexible polymer material or brittle piezoelectric ceramic. The most efficient harvesters today are capable of generating up to 10 mW of raw power during walking. Inspired by these designs a piezoelectric energy harvester made of commercially available components was developed.

The main focus in the development of the shoe energy harvester is in the design of the piezoelectric elements. When placed into a shoe they were able to generate at maximum around 1,7 mJ/step with a full bridge rectifier when using an approximate optimal resistance as the load. In addition to the piezoelectric elements, the energy harvesting circuit has an essential role in the harvester's capability to store energy. Different rectifier designs for energy harvesters are briefly discussed. This is an issue that requires further research and was not addressed in the developed energy harvester. The developed energy harvester's capability to charge various capacitors was tested. When the harvester was used to charge a supercapacitor, the energy stored per step decreased to 4,63 - 5,95 μJ/step implying that the energy harvesting circuit used is far from optimal.

With an efficient energy harvesting circuit the shoe energy harvester could provide useful power to many applications. Various wearable sensors typically consume less than 1 mW and applications that do not require continuous power can have even higher power requirements, as the generated energy can be accumulated to an energy storage and used when enough energy is available. The fact that the generated energy is located in a shoe sets certain limitations to the usage of the power. Having wires coming from the shoe to use the energy in different parts of the body seems quite impractical. Nevertheless, there are already a few demonstrations of practical applications like pedometers, pressure sensors and RFID transceivers for presence monitoring. With decreasing power requirements even GPS based applications seem realistic in the near future.

The current piezoelectric shoe energy harvesters are far from being ready for commercialization. When designing a commercial shoe energy harvester not only technologies based on piezoelectricity should be considered, as they have not been proven to be superior. However, they have proven suitable for practical applications.

8. REFERENCES

ABRAMOVICH, H., 2016. Intelligent Materials and Structures. Berlin/Boston: Walter De Gruyter.

ANTAKI, J., BERTOCCI, G., GREEN, E., NADEEM, A., RINTOUL, T., KORMOS, R. and GRIFFITH, B., 1995. A Gait-Powered Autologous Battery Charging System for Artificial Organs. ASAIO Journal, 41(3), pp. M595.

APPLE, 2018. Apple Product Information Sheet. Available from: https://images.apple.com/legal/more-resources/docs/apple-product-information-sheet.pdf [Accessed: 19.2.2018]

BENASCIUTTI D. and MORO L., 2013. Energy Harvesting with Vibrating Shoe-mounted piezoelectric cantilevers. In: Elvin N., Erturk A. (eds) Advances in Energy Harvesting Methods. Springer, New York, NY.

BHATNAGAR, V. and OWENDE, P., 2015. Energy Harvesting for Assistive and Mobile Applications. Energy Science & Engineering, 3(3), pp. 153-173.

BIONIC POWER, n.d. The PowerWalk™, Kinetic Energy Harvester. Available from: https://www.bionic-power.com/wp-content/uploads/2017/09/D0097-03_Marketing-Brochure_WEBsm.pdf [Accessed: 19.2.2018]

CAMILLONI, E., DEMASO-GENTILE, G., SCAVONGELLI, C., ORCIONI, S. and CONTI, M., 2016. Piezoelectric Energy Harvesting on Running Shoes, 2016, pp. 91-107.

CARROLL AARON and HEISER GERNOT, 2010. An Analysis of Power Consumption in a Smartphone. Proc. 2010 USENIX conf., USENIX Assoc.

CHEN, H., CONG, T.N., YANG, W., TAN, C., LI, Y. and DING, Y., 2009. Progress in Electrical Energy Storage System: A critical review. *Progress in Natural Science,* 19(3), pp. 291-312.

CHOPERENA MIKEL, 2013. RFID-powered Sensors Can Play a Big Role in the Internet of Things. RFID Journal. Available from: http://www.rfidjournal.com/articles/view?11062 [Accessed: 19.2.2018]

DU, S., JIA, Y., ZHAO, C., CHEN, S. and SESHIA, A.A., 2017. Real-world Evaluation of a Self-startup SSHI Rectifier for Piezoelectric Vibration Energy Harvesting. Sensors & Actuators: A. Physical, 264, pp. 180-187.

FAN, K., LIU, Z., LIU, H., WANG, L., ZHU, Y. & YU, B., 2017. Scavenging Energy from Human Walking Through a Shoe-Mounted Piezoelectric Harvester, Applied Physics Letters, Vol. 110(14).

FOURIE, D., 2010. Shoe Mounted PVDF Piezoelectric Transducer. Journal of Intelligent Material Systems and Structures. Available at: https://www.researchgate.net/publication/313009087_Shoe_mounted_PVDF_piezoelectric_transducer_for_energy_harvesting [Accessed: 19.2.2018]

GATTO, A. and FRONTONI, E., 2014. Energy Harvesting System for Smart Shoes, 2014 IEEE/ASME 10th International Conference on Mechatronic and Embedded Systems and Applications (MESA), IEEE, pp. 1-6.

GNS-ELECTRONICS, n.d. GNS 302uLP Ultra Low Power GPS Chip Antenna Module MT3339. Available at: http://www.gns-gmbh.com/index.php?id=282&L=1 [Accessed: 19.2.2018]

GRIFFITHS, S., 2014. These Shoes Were Made for CHARGING: Footwear generates enough power to recharge a phone as you walk. MailOnline. Available at: http://www.dailymail.co.uk/sciencetech/article-2889932/These-shoes-CHARGING-Footwear-generates-power-recharge-phone-walk.html [Accessed at: 19.2.2018]

GUAN, M.J. and LIAO, W.H., 2008. Characteristics of Energy Storage Devices in Piezoelectric Energy Harvesting Systems. Journal of Intelligent Material Systems and Structures, 19(6), pp. 671-680.

GUYOMAR, D., BADEL, A., LEFEUVRE, E. and RICHARD, C., 2005. Toward Energy Harvesting Using Active Materials and Conversion Improvement by Nonlinear Processing. IEEE Transactions on Ultrasonics, Ferroelectrics and Frequency Control, 52(4), pp. 584-595.

HARB, A., 2010. Energy harvesting: State-of-the-art. Renewable Energy, 36(10), pp. 2641-2654.

HOWELLS, C.A. (2009). Piezoelectric energy harvesting, Energy Conversion and Management, Vol. 50(7), pp. 1847-1850.

HSU, T., MANAKASETTHARN, S., TAYLOR, J.A. and KRUPENKIN, T., 2015. Bubbler: A Novel Ultra-High Power Density Energy Harvesting Method Based on Reverse Electrowetting. Scientific reports, 5, pp. 16537.

INSTEP NANOPOWER, n.d. Powering Wearable Electronics: One Step at a Time. Available at: http://www.instepnanopower.com/ [Accessed 19.2.2018]

IOP, Institute of Physics, n.d. Energy harvesting. Available at: http://www.iop.org/resources/energy/index.html [Accessed 19.2.2018]

ISHIDA, K., HUANG, T., HONDA, K., SHINOZUKA, Y., FUKETA, H., YOKOTA, T., ZSCHIESCHANG, U., KLAUK, H., TORTISSIER, G., SEKITANI, T., TOSHIYOSHI, H., TAKAMIYA, M., SOMEYA, T. and SAKURAI, T., 2013. Insole Pedometer With Piezoelectric Energy Harvester and 2 V Organic Circuits. IEEE Journal of Solid-State Circuits, 48(1), pp. 255-264.

JACKSON, N., n.d. Piezoelectric Energy Harvesting and Applications. Tyndall, National Institute. Available at: http://www.ict-energy.eu/sites/ict-energy.eu/files/Jackson_PiezoelectricEnergyHarvesting-and-Applications.pdf [Accessed 19.2.2018]

JAIN, A., K. J, P., SHARMA, A.K., JAIN, A. and P.N, R., 2015. Dielectric and Piezoelectric Properties of PVDF/PZT Composites: A review. Polymer Engineering & Science, 55(7), pp. 1589-1616.

JORDAN, T.L. and OUNATES, Z., 2001. Piezoelectric Ceramics Characterization. Technical Report. National Aeronautics and Space Administration Langley Research Center Hampton, Virginia 23681-2199.

KENDALL, J., 1998. Parasitic Power Collection in Shoe Mounted Devices. MSc Thesis. Massachusetts Institute of Technology.

KHOLKIN, A.L., PERTSEV, N.A. and GOLTSEV, A.V., 2008. Piezoelectricity and Crystal Symmetry. In SAFARI, A., AKDOGAN, E.K., Piezoelectric and Acoustic Materials for Transducer Applications. Springer-Verlag US.

KIM, H.W., BATRA, A., PRIYA, S., UCHINO, K., MARKLEY, D., NEWNHAM, R.E. and HOFMANN, H.F., 2004. Energy Harvesting Using a Piezoelectric "Cymbal" Transducer in Dynamic Environment. Japanese Journal of Applied Physics, 43(9A), pp. 6178-6183.

KIM, H., Priya, S. & UCHINO, K., 2006. Modeling of Piezoelectric Energy Harvesting Using Cymbal Transducers, Japanese Journal of Applied Physics, Vol. 45(7), pp. 5836-5840.

KUANG, Y., DANIELS A. and MEILING, Z., 2017. A Sandwiched Piezoelectric Transducer with Flex End-caps for Energy Harvesting in Large Force Environments. J. Phys. D: Appl. Phys. 50 345501.

KUTZ, M., 2016. Handbook of Measurement in Science and Engineering. 1 edn. Somerset: John Wiley & Sons, Incorporated.

KYMISSIS, J., KENDALL, C., PARADISO, J. and GERSHENFELD, N., 1998. Parasitic Power Harvesting in Shoes, 1998, pp. 132-139.

LEINONEN, M., JUUTI, J., JANTUNEN, H. and PALOSAARI, J., 2016. Energy Harvesting with a Bimorph Type Piezoelectric Diaphragm Multilayer Structure and Mechanically Induced Pre-stress. Energy Technology, 4(5), pp. 620-624.

LEKKALA, J., TUPPURAINEN, J., and PAAJANEN M., 2003. Material and Operational Properties of Large-area Membrane Type Sensors for Smart Environments. XVII IMEKO World Congress, Cavtat-Dubrovnik, 4 pp.

LEONOV, V., 2011. Energy Harvesting for Self-Powered Wearable Devices. In BONFIGLIO A. and DE ROSSI, D. Wearable Monitoring Systems. Springer US.

LI, F., XU, Z., WEI, X. and YAO, X., 2009. Determination of Temperature Dependence of Piezoelectric Coefficients Matrix of Lead Zirconate Titanate Ceramics by Quasi-static and Resonance Method. Journal of Physics D: Applied Physics, 42, pp. 095417.

LI, H., TIAN, C. and DENG, Z.D., 2014. Energy Harvesting From Low Frequency Applications Using Piezoelectric Materials. Applied Physics Reviews, 1(4), pp. 41301.

LIU Y. AND VASIC D., 2012. Self-Powered Electronics for Piezoelectric Energy Harvesting Devices, Small-Scale Energy Harvesting, Dr. Mickaël Lallart (Ed.), InTech, DOI: 10.5772/51211. Available from: https://www.intechopen.com/books/small-scale-energy-harvesting/self-powered-electronics-for-piezoelectric-energy-harvesting-devices [Accessed 19.2.2018]

LU, S. and BOUSSAID, F., 2015. An Inductorless Self-Controlled Rectifier for Piezoelectric Energy Harvesting. Sensors (Basel, Switzerland), 15(11), pp. 29192-29208.

MATEU, L. and MOLL, F., 2005. Optimum Piezoelectric Bending Beam Structures for Energy Harvesting using Shoe Inserts, Journal of Intelligent Material Systems and Structures, Vol. 16(10), pp. 835-845.

MEIER, R., KELLY, N., ALMOG, O. and CHIANG, P., 2014. A Piezoelectric Energy-harvesting Shoe System for Podiatric Sensing, 2014 36th Annual International Conference of the IEEE Engineering in Medicine and Biology Society 2014, pp. 622-625.

MISHRA, R., DURGAPRASAD, C., SAHU, S. and JAIN, S., 2015. Vibration Energy Harvesting Using Drum Harvesters. International Journal of Applied Engineering Research 10.14 (2015): 34995-35001.

MISHRA, R., JAIN, S., THAKUR, B. PAL VERMA, Q. and DURGAPRASAD, C., 2017. Performance Analysis of Piezoelectric Drum Transducers as Shoe Based Energy Harvesters International Journal of Electronics Letters, Vol. 5, Iss. 4, 2017.

MITCHESON, P.D., YEATMAN, E.M., RAO, G.K., HOLMES, A.S. and GREEN, T.C., 2008. Energy Harvesting From Human and Machine Motion for Wireless Electronic Devices. Proceedings of the IEEE, 96(9), pp. 1457-1486.

MORGAN ADVANCED MATERIALS, n.d. Physical basis. Available from: http://www.morganadvancedmaterials.com/media/4126/chapter2.pdf [Accessed 19.2.2018]

MORO, L. & BENASCIUTTI, D., 2010. Harvested Power and Sensitivity Analysis of Vibrating Shoe-mounted Piezoelectric Cantilevers, Smart Materials and Structures, Vol. 19 pp. 115011.

NIELSEN-LONN, M., HARIKUMAR, P., WIKNER, J.J. and ALVANDPOUR, A., 2015. Design of Efficient CMOS Rectifiers for Integrated Piezo-MEMS Energy-harvesting Power Management Systems, 2015, IEEE, pp. 1-4.

OTTMAN, G.K., HOFMANN, H.F., BHATT, A.C. and LESIEUTRE, G.A., 2002. Adaptive Piezoelectric Energy Harvesting Circuit for Wireless Remote Power Supply. IEEE Transactions on Power Electronics, 17(5), pp. 669-676.

OUYNAG, J., 2005. Orientation Dependence of the Piezoelectric Properties of Epitaxial Ferroelectric Thin Films, ProQuest Dissertations Publishing.

PALOSAARI, J., LEINONEN, M., HANNU, J., JUUTI, J. & JANTUNEN, H., 2012. Energy Harvesting with a Cymbal Type Piezoelectric Transducer from Low Frequency Compression, Journal of Electroceramics, Vol. 28(4), pp. 214-219.

PALOSAARI, J., LEINONEN, M., JUUTI, J. and JANTUNEN, H., 2014. Piezoelectric Circular Diaphragm with Mechanically Induced Pre-stress for Energy Harvesting. Smart Materials and Structures. 23. 085025. 10.1088/0964-1726/23/8/085025.

PALOSAARI, J., 2017. Energy Harvesting from Walking Using Piezoelectric Cymbal and Diaphragm Type Structures. Doctoral Dissertation. University of Oulu.

PANDA, P., 2017. Piezoceramic Materials and Devices for Aerospace Applications. 501-518. 10.1007/978-981-10-2134-3_23.

PAUL, P.J., TUTU, R.S.D., RICHARDS, W.K. and JEROME, V.M., 2015Project Power Shoe: Piezoelectric wireless power transfer — A mobile charging technique, 2015, IEEE, pp. 334-339.

PIEZO SYSTEMS, n.d. History of Piezoelectricity. Available from: http://www.piezo.com/tech4history.html [Accessed 22.2.2018]

PIEZO TECHNOLOGIES, n.d. An Overview of the Properties of Different Piezoceramic Materials, Technical Resource Paper. Available from: http://www.piezotechnologies.com/knowledge-desk/overview-piezo-materials [Accessed: 19.2.2018]

PILLATSCH, P., SHASHOUA, N., HOLMES, A.S., YEATMAN, E.M. and WRIGHT, P.K., 2014. Degradation of Piezoelectric Materials for EnergyHarvesting Applications. J. Physics: Conference Series 557 012129.

PLATT, S.R., FARRITOR, S., GARVIN, K. and HAIDER, H., 2005. The Use of Piezoelectric Ceramics for Electric Power Generation within Orthopedic Implants. IEEE/ASME Transactions on Mechatronics, 10(4), pp. 455-461.

RAJU M. and GRAZIER M., 2010. Energy Harvesting, ULP Meets Energy Harvesting: A game-changing combination for design engineers. Available from: http://www.ti.com/lit/wp/slyy018a/slyy018a.pdf [Accessed 19.2.2018]

RAMADASS, Y.K. and CHANDRAKASAN, A.P., 2010. An Efficient Piezoelectric Energy Harvesting Interface Circuit Using a Bias-Flip Rectifier and Shared Inductor. IEEE Journal of Solid-State Circuits, 45(1), pp. 189-204.

REN, B., OR, S.W., ZHAO, X.Y. & LUO, H.S., 2010. Energy Harvesting Using a Modified Rectangular Cymbal Transducer Based on 0.71Pb(Mg1/3Nb2/3)O-3-0.29PbTiO(3) Single Crystal, Journal of Applied Physics, Vol. 107(3).

ROCHA, J.G., GONCALVES, L.M., ROCHA, P.F., SILVA, M.P. and LANCEROS-MENDEZ, S., 2010. Energy Harvesting From Piezoelectric Materials Fully Integrated in Footwear. IEEE Transactions on Industrial Electronics, 57(3), pp. 813-819.

ROGERS, C.A. and WALLACE, G.G., Dec 31, 1994. Second International Conference on Intelligent Materials: Proceedings, Dec 31, 1994.

ROUNDY, S.J., 2003. Energy Scavenging for Wireless Sensor Nodes with a Focus on Vibration to Electricity Conversion, ProQuest Dissertations Publishing.

SCHLINGLOFF H., 2014. Low Power Wireless Standarts. Humboldt-Universität zu Berlin, Institut für Informatik. Available from: https://www2.informatik.hu-berlin.de/~hs/Lehre/2014-WS_SP-CPS/20141028_Low-Power-Wireless-Standards_1.pdf [Accessed 19.2.2018]

SHENCK, 1999. A Demonstration of Useful Electric Energy Generation from Piezoceramics in a Shoe, MSc Thesis. Massachusetts Institute of Technology.

SHENCK, N.S. and PARADISO, J.A., 2001. Energy Scavenging with Shoe-mounted Piezoelectrics. IEEE Micro, 21(3), pp. 30-42.

SNEHALIKA and BHASKER, M.U., 2016. Piezoelectric Energy harvesting from shoes of Soldier, 2016, IEEE, pp. 1-5.

STARNER, T. and PARADISO, J. A, 2004 Human Generated Power for Mobile Electronics. Low Power Electronics Design, volume 45. CRC Press, 2004.

SODANO, H.A., INMAN, D.J. and PARK, G., 2005. Comparison of Piezoelectric Energy Harvesting Devices for Recharging Batteries. Journal of Intelligent Material Systems and Structures, 16(10), pp. 799-807.

TOLENTINO, I.M. and TALAMPAS, M.R., 2012. Design, Development, and Evaluation of a Self-powered GPS Tracking System for Vehicle Security, 2012, IEEE, pp. 1-4.

UCHINO K., 2000. Ferroelectric Devices. Marcel Dekker, Inc.

UCHINO K., 2010 The Development of Piezoelectric Materials and the New Perspective. In UCHINO K., Advanced Piezoelectric Materials. Woodhead Publishing Limited.

VULLERS, R.J.M., VAN SCHAIJK, R., DOMS, I., VAN HOOF, C. and MERTENS, R., 2009. Micropower Energy Harvesting. Solid State Electronics, 53(7), pp. 684-693.

WANG, 2010. Piezoelectric Energy Harvesting Utilizing Human Locomotion, MSc Thesis, University of Minnesota.

WANT, R., HOPPER, A., FALCÃO, V. and GIBBONS, J., 1992. The Active Badge Location System. ACM Transactions on Information Systems (TOIS), 10(1), pp. 91-102.

WANG, S., CHAN, H., SUN, C., LAM, K., GUO, M., KWOK, K. & ZHAO XING-ZHONG, 2007. Energy Harvesting with Piezoelectric Drum Transducer, Applied Physics Letters, Vol. 90(11), pp. 3.

WENDT, J.B., GOUDAR, V., NOSHADI, H. and POTKONJAK, M., 2012. Spatiotemporal assignment of energy harvesters on a self-sustaining medical shoe, 2012, IEEE, pp. 1-4.

WISCKE, M. and WOIAS, P., 2007. Power Harvesting from Human Walking. Proc. PowerMEMS 2007, pages: 65 - 68.

ZHAO, J.J. and YOU, Z., 2014. A Shoe-Embedded Piezoelectric Energy Harvester for Wearable Sensors, SENSORS, Vol. 14(7), pp. 12497-12510.